Universität St.Gallen

Are classical option pricing models consistent with observed option second-order moments? Evidence from high-frequency data

Francesco Audrino, Matthias Fengler

August 2013 Discussion Paper no. 2013-11

School of Economics and Political Science, Department of Economics

University of St. Gallen

Editor: Martina Flockerzi
University of St. Gallen
School of Economics and Political Science
Department of Economics
Bodanstrasse 8
CH-9000 St. Gallen
Phone +41 71 224 23 25
Fax +41 71 224 31 35
Email seps@unisg.ch

Publisher: School of Economics and Political Science
Department of Economics
University of St. Gallen
Bodanstrasse 8
CH-9000 St. Gallen
Phone +41 71 224 23 25
Fax +41 71 224 31 35

Electronic Publication: http://www.seps.unisg.ch

Are classical option pricing models consistent with observed option second-order moments? Evidence from high-frequency data[1]

Francesco Audrino, Matthias Fengler

Authors' addresses:

Prof. Dr. Francesco Audrino
Institute of Mathematics and Statistics
Bodanstrasse 6
CH-9000 St. Gallen
Phone +41 71 224 24 31
Fax +41 71 224 28 94
Email francesco.audrino@unisg.ch
Website http://www.mathstat.unisg.ch/People.aspx

Prof. Dr. Matthias Fengler
Institute of Mathematics and Statistics
Bodanstrasse 6
CH-9000 St. Gallen
Phone +41 71 224 24 57
Fax +41 71 224 28 94
Email matthias.fengler@unisg.ch
Website http://www.mathstat.unisg.ch/People.aspx

[1] We thank Yujia Hu, Andreas Kaeck, Simon Knaus, and seminar participants at CFE 2012 (Oviedo) and at St. Gallen University for many useful comments and suggestions. We also thank Jonas Hein for support with extracting and organizing the data. Both authors gratefully acknowledge financial support from the Swiss National Science Foundation (Grant 144033: ``Analysis and models of cross asset dependency structures in high-frequency data.")

Abstract

We suggest a joint analysis of ex-post intra-day variability in an option and its associated underlying asset market as a means of validating an option pricing model. For this purpose, we contrast option realized variance with the realized variance that would be implied from the underlying asset price path under certain model assumptions. In the empirical analysis, we first focus on the implied volatility compensated Black-Scholes model and the Heston model. Corroborating findings presented in the literature for first-order moments and option data of lower frequency, we find substantial deviations between both markets. Options second-order moments are significantly closer to the realized ones, after controlling for the presence of jumps and after recalibrating the Heston model every day. This highlights the relevance of jumps and more sophisticated underlying's stochastic volatility dynamics also from an option's second-order moment perspective.

Keywords

Option pricing, high frequency data, realized variance, stochastic volatility.

JEL Classification

C52, C58, G13, G17.

1 Introduction

There are two basic tenets in option pricing theory: (*i*) the risk-neutral expectation of the underlying asset's integrated variance is a key determinant of an option's price; (*ii*) the efficacy of an option's hedge critically depends on the variance of the underlying asset realized along its path, i.e. its so-called realized variance. Since high-frequency data first became available, much research has consequently been devoted to characterizing, modeling, and forecasting realized variance as measured in major underlying asset classes such as stocks, indices, futures and foreign exchange rates.[1] Insights from this research substantially improved our understanding of these markets and ultimately lead to the development of more refined option pricing models. For option pricing, for instance, a typical approach would be to employ realized variance estimated from intra-day sampled returns on the underlying asset to improve on the state recovery of latent volatility at a daily frequency; see Bollerslev and Todorov (2011), Andersen et al. (2012), Christoffersen et al. (2012), and Corsi et al. (2013).

In the present work, rather than using intra-day data as a tool for an analysis at a lower frequency, we study high-frequency dynamics in the underlying asset and its associated option market in concert. For this purpose, we introduce the notion of option realized variance. Like the usual concept, option realized variance is the cumulative variance realized by the sample path of successive option price observations. We then relate the observed option realized variance on the one hand with the realized variance that would be implied from the underlying asset price path under certain model assumptions on the other. Ideally, both quantities should yield similar estimates. Any mismatch therefore allows conclusions to be drawn on misspecification of the option pricing model from the perspective of option second-order moments. A joint analysis of realized variance in underlying asset and option markets therefore serves as a novel means of validating an

[1] See, among others, Andersen, Bollerslev, Diebold and Ebens (2001), Andersen, Bollerslev, Diebold and Ebens (2001), Andersen et al. (2003), Barndorff-Nielsen and Shepard (2001a), Barndorff-Nielsen and Shepard (2001b), Barndorff-Nielsen and Shepard (2002), and more recently, Todorov and Tauchen (2011) and Todorov et al. (2011).

option pricing model.

Options are a nonlinear function of the underlying asset price. Unlike realized variance of delta-one instruments, such as stocks and futures, option realized variance therefore is a complicated functional of the underlying asset's realized path. Moreover, aside from the underlying itself, option realized variance may involve realized variance contributions from additional risk factors, such as latent volatility factors. These facts may render such a study intricate, but are not necessarily prohibitive. Here, we demonstrate the potential of this analysis by focusing on the two primary workhorses of the financial literature: the implied volatility compensated Black and Scholes (1973) model and the Heston (1993) model.

For our study we use high-frequency intra-day transaction records of put and call options written on the EURO STOXX 50® index sampled between 2003-2011. The EURO STOXX 50® is the leading financial market indicator in the Eurozone. Options and futures written on this index belong to the most heavily traded derivatives in Europe. Thanks to the liquidity of this market, we are able to compute accurate and reliable measures for the daily second-order moments of option prices. We then ask whether and under which circumstances these classical one- and two-factor models for the underlying asset price are able to reproduce the variance dynamics observed in the option market.

Our results can be summarized as follows. First, option realized volatility predictions obtained assuming the implied volatility compensated Black-Scholes or the Heston model are systematically inconsistent with the observed option realized volatilities. The richer flexibility allowed by stochastic volatility, although generally improving the Black-Scholes predictions, is not enough to obtain variance predictions that are in line with the observed ones. This result is irrespective of whether we consider put or call options with different characteristics (i.e., moneyness and time to maturity), different frequencies, different time periods, or whether we exclude days in which fundamental model assumptions are violated. Moreover, differences between the realized volatility series are significantly larger than those we obtain in simulations. As a consequence, they may not be (completely) ascribed to numerical errors unavoidably related to the approximations. Second, regressing observed second-order moments on model-based ones, we show that the predictions based on the Heston model are on average too high, yielding an overestimation of the true risk (associated with second-order moments) realized in the option market. In contrast, predictions obtained assuming the Black-Scholes model for the underlying index price are on average too large (small) for call (put) options. Third, in analyzing the time series of differences between observed and model-based second-order moments, and in particular looking at the different time periods, the sign of the differences is systematically different for call and put options when assuming the Heston model for the underlying index dynamics: During periods characterized by low uncertainty and stable market conditions, second-order moments of call (put) options are underestimated (overestimated). The opposite holds true during highly volatile periods (mainly during and after the financial crisis). Fourth, we find a distinct segregation in the approximation quality between put and call markets. In particular, we find that second-order moments of calls are captured markedly more poorly than those of puts.

In conclusion, both models fail to reproduce observed option second-order moments, with the Heston model moderately outperforming the Black-Scholes model. Our results provide a rationalization from the viewpoint of ex-post intra-day variability of option prices for the deficiencies of those models that have been previously documented in the literature. In particular, they point to the existence of additional relevant pricing factors that affect option second-order moments. We thus add from an intra-day perspective to similar findings that were discovered in option data at lower frequencies, as discussed e.g. in Poteshman (2001), Bollen and Whaley (2004), or Han (2008).

Our research of option second-order moments is related to the option pricing literature in various ways. Perhaps closest in spirit is Bakshi et al. (2000a). In that study, intra-day dynamics of quoted option prices are studied in order to discriminate between one- versus two-dimensional factor models as a description of the underlying asset price dynamics. Furthermore, the examination of option second order moments can be understood as a special type of hedging analysis, such as in Bakshi et al. (1997) and Dumas et al. (1998), with the important qualification that the joint analysis of option and underlying-based realized variance considers only first-order intra-day effects. This is because higher-order effects on option prices, such as gamma, or smooth effects, including time decay, are necessarily ignored by a realized variance analysis. Moreover, it may only focus on short-term aspects of the performance, since only options with the highest liquidity may enter the analysis. It will usually not be possible to track a distinct option with a fixed strike and expiry date over a period longer than a single trading day as one would typically do when studying the hedging performance. And finally, one may read this work as adding a second-order moment perspective to the asset pricing literature exploring the cross-sectional distribution of option returns. Examples of this analysis of first-order moments of option returns include Coval and Shumway (2001), Jones (2006), and Constantinides et al. (2011).

The rest of the paper is organized as follows. Section 2 develops the theory and provides the main formulas needed to compute option second moments. In Section 3 we sketch the theory on realized volatility and discuss its properties as an estimator of the unobservable option quadratic variation. Monte Carlo simulations are provided. In Section 4, we describe the data and construct the different (i.e., observed and model-based) realized variance series under investigation. Sections 5 and 6 present the main empirical results. Concluding remarks are offered in Section 7.

2 Options second-order moments

In this section, we derive the second-order properties of the option price dynamics. We consider the case in which the underlying asset price follows a one-dimensional diffusion process. As an extension, we also study a two-dimensional diffusion process, in which the second state variable is return volatility.

2.1 One-dimensional diffusion model

Consider a European-style call option with strike price K and τ years to expiration, written on some non-dividend-paying asset whose time t (log-)price is denoted by $y(t)$.

To do so, we first specify the process followed by $y(t)$ and the valuation rule for the option. In a second step, using the mathematical theory developed for stochastic processes, we can analytically derive the second-order properties of the options dynamics.

2.1.1 Basic model framework

On filtered probability space $(\Omega, \mathcal{F}, P, (\mathcal{F}(t))_{t\geq 0})$, assume that $y(t)$ follows the one-dimensional diffusion

$$dy(t) = \alpha(t)dt + \sigma(t)dw_1(t), \;\; t \geq 0, \tag{1}$$

where $y(0) > 0$ and $w_1(t)$ is a standard Brownian motion. Throughout we assume that the following conditions on the drift $\alpha(t)$ and volatility functions $\sigma(t)$ hold with probability one:

(*i*) $\alpha(t)$ is continuous (and thus predictable) and has locally finite variation paths;

(*ii*) $\sigma(t)$ is càdlàg, locally bounded away from zero and has locally squared integrable sample paths.

Under these assumptions $y(t)$ is a semimartingale and volatility is allowed to display a wide range of patterns. Many option pricing models introduced in the literature satisfy these assumptions, such as the Black-Scholes (BS) model with a constant as volatility function, the Cox and Ross (1976) constant elasticity of variance model, and the general local volatility model by Dupire (1994).

Assume that the financial market admits no free lunches. By the fundamental theorem of asset pricing there exists a measure under which the discounted underlying price process is a martingale (Dalang et al.; 1990). This allows pricing derivatives as discounted expected payoffs. Let $C(t, S, \tau, K)$ and $P(t, S, \tau, K)$ denote the time-t price of a call and a put option; then

$$C(t, S, \tau, K) \;\; = \mathrm{E}_t^*[e^{-r\tau} \max\{S(t+\tau) - K, 0\}] \tag{2}$$

$$P(t, S, \tau, K) \;\; = \mathrm{E}_t^*[e^{-r\tau} \max\{K - S(t+\tau), 0\}] \tag{3}$$

where the time-t conditional expectation operator $\mathrm{E}_t^*[\cdot]$ is with respect to a martingale measure equivalent to P. Furthermore, $S = e^y$ is the price of the underlying asset, and r is the spot interest rate which will be assumed to be constant for the sake of simplicity.

We now derive the price dynamics of the logarithm of the call option (2). Similar results can be obtained for put options. Suppressing dependence on τ and K define

$$X(t, y) = \log(C(t, S)) = \log(C(t, e^y)) \; . \tag{4}$$

By use of Ito's lemma, we get

$$dX = \left\{ X_t + \frac{1}{2}\sigma^2(t) X_{yy} \right\} dt + X_y dy \; , \tag{5}$$

where the subscripts on X stand for the respective partial derivatives. Note that the process (5) is a semimartingale and its drift and volatility functions satisfy the same regularity conditions we stated for (1). By using the definition in (4), we get

$$X_y = X_C \frac{\partial C}{\partial y} = \frac{S}{C}\frac{\partial C}{\partial S} = \frac{S}{C}\Delta_C =: \tilde{\Delta}_C \; , \tag{6}$$

where $\Delta_C = \frac{\partial C}{\partial S}$ is the delta of the call option, measuring the sensitivity of the option to changes in the underlying. The delta of the log-call price $\tilde{\Delta}_C$ is also known as the elasticity of the option. Under our model assumptions and assuming that time-to-maturity of the option is not equal to zero, elasticity is bounded. In particular, Bergman et al. (1996) have shown that

$$1 \leq \tilde{\Delta}_C \leq 1 + \frac{\text{constant}}{C} \; .$$

The elasticity weight is crucial for determining option second-order moment dynamics as will be seen presently.

2.1.2 Quadratic variation and option variance dynamics

One of the most important properties of semimartingales as introduced in (1) is that the second order moments can be characterized by the quadratic variation process; see, for example, Jacod and Shiryaev (1987), p. 55. It is defined as

$$[y](t) = p - \lim_{M \to \infty} \sum_{i=1}^{M} \big(y(t_i) - y(t_{i-1}) \big)^2$$

where $p-\lim$ denotes the limit in probability under the physical measure P and $t_0 = 0 < t_1 < t_2 < \ldots < t_M = t$ is any sequence of partitions such that $\sup_i(t_i - t_{i-1}) \to 0$ when $M \to \infty$.

Under the general assumptions made for the process (1), the quadratic variation of y equals the integrated variance of the instantaneous returns (see Barndorff-Nielsen and Shepard, 2004, among others), i.e.,

$$[y](t) = \int_0^t \mathrm{Var}(dy(u) \mid \mathcal{F}(u)) = \int_0^t \mathrm{Var}(\sigma(u)dw_1(u) \mid \mathcal{F}(u)) = \int_0^t \sigma^2(u)du\ , \tag{7}$$

where $\mathcal{F}(u)$ is the natural filtration of $y(u)$. The last equality follows by $[w_1](t) = t$.

Applying quadratic variation theory to the log-call price process (5) we get

$$[X](t) = \int_0^t \mathrm{Var}(dX(u) \mid \mathcal{F}(u)) = \int_0^t \tilde{\Delta}_C^2\ \sigma^2(u)du =: I_1, \tag{8}$$

where $\tilde{\Delta}_C$ is given in (6).

In the empirical analysis performed in the next sections we will estimate the options (weighted) integrated variance in two ways: (i) directly from intra-day option data and (ii) from intra-day observations of the underlying asset along with a model assumption on the option delta. We then test their mutual compatibility. To appreciate this strategy note that even though the options are priced under the risk-neutral measure, their sampled returns and hence their quadratic variation in (8) are observed under the physical measure.

2.2 Extending the model: stochastic volatility

2.2.1 Basic model framework

We now extend the underlying asset price dynamics to allow for stochastic volatility.[2] In addition to the underlying log-price process given in (1), assume that its squared spot volatility denoted by $V(t) = \sigma^2(t)$ follows a second diffusion process

$$dV(t) = m(t)dt + \theta(t)dw_2(t),\ t \geq 0\ , \tag{9}$$

[2]The literature on stochastic volatility models is discussed by, among others, Harvey et al. (1994), Taylor (1994), Ghysels et al. (1996), Shepard (1996), and Kim et al. (1998).

where the functions $m(t)$ and $\theta(t) > 0$ satisfy the usual regularity conditions such that the assumptions stated for $\sigma(t)$ in Section 2.1.1 are fulfilled. $w_2(t)$ denotes a second standard Brownian motion that may be correlated to $w_1(t)$ with constant correlation parameter ρ. This set-up includes, but is not limited to, the models by Hull and White (1987), Scott (1987), and Heston (1993).

As the log-call price X now depends on both stochastic processes y and V, i.e.,

$$X(t, y, V) = \log(C(t, S, V)) = \log(C(t, e^y, V)) \ , \tag{10}$$

it follows from Ito's lemma that

$$dX = Fdt + X_y dy + X_V dV \ . \tag{11}$$

By F we denote a sum of factors which are multiplied with dt and which therefore are irrelevant to the option's quadratic variation $[X](t)$. As before X_y is the elasticity of the call option $\tilde{\Delta}_C$, see (6), whereas X_V is a weighted measure of the variance vega of the option price, i.e., its sensitivity to changes in the underlying's stochastic variance. Denoting the variance vega by ν we have that

$$X_V = X_C \frac{\partial C}{\partial V} = \frac{1}{C} \cdot \nu_C =: \tilde{\nu}_C \tag{12}$$

The two elasticity factors ($\tilde{\Delta}_C$ and $\tilde{\nu}_C$) are crucial to determining options second order moments. Aside from requiring that time-to-maturity of the option not reaches zero, the additional assumptions on the drift and diffusion function of the stochastic volatility process V such that $\tilde{\Delta}_C$ is bounded are stated in Bergman et al. (1996), Theorem 3: (a) the drift and diffusion of the risk neutralized process for $V(t)$ are not allowed to depend on the level of $y(t)$; and (b) the covariance between instantaneous percent changes in $y(t)$ and changes in $V(t)$ does not depend on the level of $y(t)$. For the Heston model as well as for many other stochastic volatility models considered in the literature, these assumptions are satisfied. The fact that $\tilde{\nu}_C$ is bounded follows directly from the integrability of $V(t) = \sigma^2(t)$.

2.2.2 Quadratic variation and option variance dynamics

Let us assume that the integrated variance process exists, i.e., $\int_0^t \sigma^2(u)du < \infty$ for all $t < \infty$. In that case the quadratic variation theory extends to stochastic volatility models. For the two-dimensional diffusion process (1) together with (9) we have

$$[y](t) = \int_0^t \sigma^2(u)du \tag{13}$$

exactly as in (7).

Let us now apply the quadratic variation theory to the log-call price process derived in (11). From the polarization identity[3] we get

$$\begin{aligned}
[X](t) &= \int_0^t \operatorname{Var}(dX(u) \mid \mathcal{F}(u)) \\
&= \int_0^t X_y^2 \operatorname{Var}(dy(u) \mid \mathcal{F}(u)) + \int_0^t X_V^2 \operatorname{Var}(dV(u) \mid \mathcal{F}(u)) \\
&\quad + 2\int_0^t X_y X_V \operatorname{Cov}(dy(u), dV(u) \mid \mathcal{F}(u)) \ ,
\end{aligned} \tag{14}$$

where the last integral denotes (without considering the product $X_y X_V$) the quadratic covariation between the diffusion processes y and V defined as

$$[y,V](t) = p - \lim_{M\to\infty} \sum_{i=1}^{M} (y(t_i) - y(t_{i-1})(V(t_i) - V(t_{i-1})$$

where $t_0 = 0 < t_1 < t_2 < \ldots < t_M = t$ is any sequence of partitions such that $\sup_i(t_i - t_{i-1}) \to 0$ when $M \to \infty$.

Using the results computed in (6) and (12) we get

$$\begin{aligned}
[X](t) &= \int_0^t \tilde{\Delta}_C^2 \, \sigma^2(u)du + \int_0^t \tilde{\nu}_C^2 \theta^2(u)du + 2\int_0^t \tilde{\Delta}_C \tilde{\nu}_C \rho\sigma(u)\theta(u)du \\
&=: I_1 + I_2 + 2I_3 \ ,
\end{aligned} \tag{15}$$

[3] In the quadratic variation theory, the polarization identity allows one to compute the quadratic variation of a sum of two stochastic processes, say Y and Z, by introducing the quadratic covariation $[Y,Z](t)$ as

$$[Y + Z](t) = [Y](t) + [Z](t) + 2[Y,Z](t) \ ,$$

provided that all quantities exist; see e.g., Karatzas and Shreve (1991) or Protter (2005).

where I_1 is the same term we obtained when computing the quadratic variation of the log-call price process in the one-dimensional diffusion case. The two additional factors are due to the second diffusion process. Noting that I_1 and I_2 are positive, more attention must be devoted to I_3. First, there is strong empirical evidence that correlation ρ is negative. This fact is called leverage in the financial literature. Second, for options of different types (i.e., call or put options), the sign of the product $X_y X_V$ is different. For call options both derivatives are positive, whereas for put options $\Delta_P < 0$ and $\nu_P > 0$. This results in a negative sign of the product. Therefore, the contribution of I_3 to the total quadratic variation of X is positive for a put and negative for a call.

2.3 Considerations of model-dependence

On casual inspection, one could think that the first integral term I_1 in (8) is the same or at least very close to I_1 in (15). Such a conclusion, however, may be naïve. Note that an observed market call price can always be approximated by an implied volatility compensated BS price. Hence, we get for its delta

$$\Delta_C = \Delta_C^{BS} + \nu_\sigma^{BS} \frac{\partial \hat{\sigma}}{\partial S} \, . \tag{16}$$

Thus, the true delta is a BS delta corrected by the BS-volatility vega times a term that describes how implied volatility evolves with the underlying dynamics. Models may differ in this respect. For instance, if we additionally assume that $S(t)$ is independent from its unit of measurement[4], such as in the Heston model, it follows that implied volatility is homogeneous of degree zero in strike and spot price. Applying the Euler theorem to implied volatility we therefore get

$$\Delta_C = \Delta_C^{BS} - \nu_\sigma^{BS} \frac{K}{S} \frac{\partial \hat{\sigma}}{\partial K} \, , \tag{17}$$

which relates the amount of the correction to the implied volatility skew. As a consequence, in particular in periods when the implied volatility skew is pronounced, the

[4]This property is sometimes referred to as scale-invariance; see Renault (1997), Bates (2005) and Alexander and Nogueira (2007) for a detailed account.

correction term may be substantial and Δ_C^{BS} may be far away from the true delta. This fact can result in differences between the I_1 factors in (8) and the one derived under alternative assumptions as in (15). As we will show in our empirical investigation, this difference can be large.

Similar considerations of model dependence apply to the variance vega. Thus alternate model assumptions drive a wedge between the observed option second-order moments and the model-based approximations using underlying data and form the basis for testable predictions of model misspecification.

2.4 Testable predictions of model misspecification

The accuracy of model-based option second-order moments (8) and (15) is directly testable using properly sampled option data in connection with the observed data on the underlying index. The two predictions to be tested here are the following:

(*i*) In the one-dimensional diffusion setting, every day t the observed options second moments should be compatible with the ones obtained using data of the underlying asset and a model-based estimator of the quadratic variation derived in (8).

(*ii*) In the two-dimensional stochastic volatility setting, every day t the observed options second moments should be compatible with the ones obtained using data of the underlying asset and a model-based estimator for the sum of the three factors in the quadratic variation expression derived in (15).

These predictions examine whether using model-based estimators for the options second moments are able to reproduce the reality of observed option second-order moments. Because of their widespread use in academia and private institutions, we use the BS model and the Heston model to represent one-dimensional and two-dimensional processes, respectively, in the empirical analysis. The required estimation theory is well-known and summarized in the next section.

3 Realized variance

In this section, we sketch the properties of the realized variance as an estimator of the quadratic variation. This will allow us to estimate in an accurate way the terms in the model-based options second-order moments.

3.1 Definition and properties

Suppose that we record the log-prices $y_{j,t}$, $j = 1, \ldots, M$, of an asset, such as a stock price, at M equally spaced time points during the day t. Define the intra-day high-frequency returns $r_{j,t}$ for day t as

$$r_{j,t} = y\Big(t - 1 + \frac{j}{M}\Big) - y\Big(t - 1 + \frac{j-1}{M}\Big),\ j = 1, \ldots, M.$$

Clearly, $r_t = \sum_{j=1}^{M} r_{j,t}$, where $r_t = y(t) - y(t-1)$ denotes the daily return on day t.

We now recall the well-known connection between realized variance $RV_y(t)$ defined as

$$RV_y(t) = \sum_{j=1}^{M} r_{j,t}^2 \tag{18}$$

and quadratic variation.[5] The main result states that if y is a semimartingale with drift and volatility functions satisfying the assumptions stated in Section 2.1.1, realized variance consistently estimates the daily increments of the quadratic variation:

$$RV_y(t) = \sum_{j=1}^{M} r_{j,t}^2 \xrightarrow{P} [y](t) - [y](t-1) = \int_{t-1}^{t} \sigma^2(u)du\ . \tag{19}$$

This result also holds in the case that $\sigma(t)$ is a stochastic volatility process under the additional provision that the integrated variance process exists. It holds irrespectively of the stochastic relation between the drift function α, the volatility function σ, and the Brownian motion w_1 in (1).

[5] Realized variances have been used for a long time in the financial literature and their properties have been extensively studied, for example, by Andersen, Bollerslev, Diebold and Ebens (2001), Andersen, Bollerslev, Diebold and Labys (2001), Barndorff-Nielsen and Shepard (2001b), Barndorff-Nielsen and Shepard (2001a), and Barndorff-Nielsen and Shepard (2002). We refer to Andersen et al. (2010) for a good survey of this field, including a discussion of the related literature.

3.2 Application to options quadratic variation

To obtain a consistent estimator of $\int_{t-1}^{t} \tilde{\Delta}_C^2\ \sigma^2(u)du$ we will apply a (weighted) realized variance estimator. To this end, let us denote by

$$\tilde{\alpha}(t) = \tilde{\Delta}_C\ \alpha(t) = \frac{S(t)}{C(t, S(t))} \frac{\partial C(t, S(t))}{\partial S(t)} \alpha(t)$$
$$\tilde{\sigma}(t) = \tilde{\Delta}_C\ \sigma(t) = \frac{S(t)}{C(t, S(t))} \frac{\partial C(t, S(t))}{\partial S(t)} \sigma(t)$$

transformed drift and volatility functions using $\tilde{\Delta}_C$ as weight. Since these functions fulfill the assumptions stated for the original drift and volatility functions in Section 2, we can introduce a weighted log-price stochastic process $\tilde{y}(t)$ and exploit the connection between realized variance and quadratic variation on it.

Let $d\tilde{y}(t) = \tilde{\Delta}_C dy(t)$ be defined as

$$d\tilde{y}(t) = \tilde{\alpha}(t)dt + \tilde{\sigma}(t)dw_1(t),\ t \geq 0\ ,$$

with $\tilde{y}(0) > 0$ and drift and volatility functions defined above. Then the realized variance computed using the weighted intra-day returns

$$\tilde{r}_{j,t} = \tilde{\Delta}_C \Big[y\Big(t - 1 + \frac{j}{M}\Big) - y\Big(t - 1 + \frac{j-1}{M}\Big)\Big],\ j = 1, \ldots, M,$$

where $\tilde{\Delta}_C = \tilde{\Delta}_C\Big(t - 1 + \frac{j-1}{M}\Big)$, is a consistent estimator for the daily increments of the quadratic variation of the transformed process $\tilde{y}$

$$dRV_{\tilde{y}}(t) = \sum_{j=1}^{M} \tilde{r}_{j,t}^2 = \hat{I}_1 \xrightarrow{P} [\tilde{y}](t) - [\tilde{y}](t-1) = \int_{t-1}^{t} \tilde{\sigma}^2(u)du = \int_{t-1}^{t} \tilde{\Delta}_C^2\ \sigma^2(u)du \quad (20)$$

that is the quantity we are interested in. We term it dRV, as it is a model-derived realized variance estimator.

To compute dRV using the transformed process, we discretize $\tilde{\Delta}_C$ at time $t - 1 + \frac{j-1}{M}$, that is at the beginning of each intra-day interval, strictly following the definition of the Ito integral. For comparison purposes, we also employ three other choices:

- evaluate $\tilde{\Delta}_C$ at the end of the intra-day intervals (i.e., at $t - 1 + \frac{j}{M}$);

- combine both schemes conditionally on whether the intra-day return is positive or negative. This allows us to obtain upper and lower bounds for the whole integral $\hat{I}_1$.

As we will show in Section 5.2, these alternative discretization choices will hardly change the estimates.

To test whether the options second-order moments obtained in the different settings (i.e., one-dimensional and two-dimensional stochastic volatility diffusion models) match the second-order moments observed in the option market, we compare the model-derived quantities with realized variances computed from intra-day option data. We denote these observed options realized variances by oRV. They are computed by means of

$$oRV_X(t) = \sum_{j=1}^{M} \left[X\left(t - 1 + \frac{j}{M}\right) - X\left(t - 1 + \frac{j-1}{M}\right)\right]^2$$

in a model-free setting, only assuming standard regularity conditions on the process X such that the properties of the realized variance estimator are fulfilled.

3.3 Estimation of additional quadratic variation terms in the stochastic volatility model: the Heston case

In the stochastic volatility setting we have to cope with two additional terms arising from the quadratic variation of the volatility process and the covariation of the volatility and the underlying asset price process. Both terms require not only knowledge of a delta but also a vega. In order to be able to proxy these quantities, we specialize to the Heston model. In this case, (9) specializes to a Cox-Ingersoll-Ross process with $m(t) = \kappa(\lambda - V(t))$ and $\theta(t) = \xi\sqrt{V(t)}$, where κ is the rate at which $V(t)$ approaches its long-run mean λ, and ξ is its volatility coefficient. Inserting we obtain

$$I_2 = \int_0^t \tilde{\nu}_C^2 \theta^2(u) du \quad = \quad \xi^2 \int_0^t \left(\frac{\nu_C}{C}\right)^2 \sigma^2(u) du \tag{21}$$

$$I_3 = \rho \int_0^t \tilde{\Delta}_C \tilde{\nu}_C \sigma(u)\theta(u) du \quad = \quad \rho\xi \int_0^t \frac{\tilde{\Delta}_C \nu_C}{C} \sigma^2(u) du \; . \tag{22}$$

Following the ideas outlined in Section 3.2, we consider the transformed processes

$$d\tilde{y}_2(t) = \tilde{k}_2 dy(t) \tag{23}$$

$$d\tilde{y}_3(t) = \tilde{k}_3 dy(t) \tag{24}$$

where $\tilde{k}_2 = \frac{\nu_C}{C}$ and $\tilde{k}_3 = \sqrt{\frac{\tilde{\Delta}_C \nu_C}{C}}$.[6] As before, realized variance is computed using the weighted intra-day returns

$$\tilde{r}_{j,t;i} = \tilde{k}_i \Big[y\Big(t-1+\frac{j}{M}\Big) - y\Big(t-1+\frac{j-1}{M}\Big)\Big],\ j = 1,\dots,M,$$

with $\tilde{k}_i = \tilde{k}_i\Big(t-1+\frac{j-1}{M}\Big)$ and $i = 2,3$. As estimators we obtain

$$RV_{\tilde{y}_2}(t) = \hat{I}_2 = \hat{\xi}^2 \sum_{j=1}^{M} \tilde{r}^2_{j,t;2} \approx \xi^2 \int_{t-1}^{t} \frac{\nu_C^2}{C^2} \sigma^2(u) du \tag{25}$$

and

$$RV_{\tilde{y}_3}(t) = \hat{I}_3 = \hat{\rho}\hat{\xi} \sum_{j=1}^{M} \tilde{r}^2_{j,t;3} \approx \rho\xi \int_{t-1}^{t} \frac{\tilde{\Delta}_C \nu_C}{C} \sigma^2(u)\ du\ , \tag{26}$$

where $\hat{\rho}$ and $\hat{\xi}$ denote the estimates obtained from the Heston calibration. For the computation of the different elasticity factors in (20), (21), and (22), we use model-based greeks and observed option prices. As above we denote the model-derived RV by

$$dRV = \hat{I}_1 + \hat{I}_2 + 2\hat{I}_3\ .$$

3.4 Simulations

In this section, we investigate the properties of oRV estimators in an idealized simulation framework, the design of which imitates our empirical setting. We simulate both the BS and the Heston model. In either case, we simulate the underlying paths and price options. We then compare the accuracy of the RV estimates by regressing oRV on its underlying implied approximations dRV according to (20) and the sum of the three terms introduced in (20), (25), and (26), respectively. Interest rates and dividends are assumed to be zero.

[6]For the puts, since $\Delta_P < 0$, we necessarily have $\tilde{k}_3 = \sqrt{\left|\frac{\tilde{\Delta}_P \nu_P}{P}\right|}$ and $(-1)RV_{\tilde{y}_3}(t)$ below. By local boundedness of σ (introduced in Section 2.1), we ensure that $\tilde{k}_2$ and $\tilde{k}_3$ are (locally) bounded, and hence the asymptotic properties of the RV estimators are preserved.

3.4.1 Description of simulation framework

For each run, the model is simulated over 250 trading days in five, 15 and 30 minutes intra-day increments. Initially, a put and a call option with 35 days to expiry are issued. In line with the empirical analysis, option strikes are chosen slightly OTM, i.e., we take $X_P = (1-a)S_0$ for the put and for the call $X_C = (1+a)S_0$ with $a = 2.5\%$ and $S_0 = 100$. Throughout a trading day the option strikes remain unchanged. Before a new trading day starts, however, options are restriked by the same factor using the "opening price" of the underlying; the opening price is identical to the previous day's settlement price. Restriking is done to preserve the moneyness characteristics of the options over the different simulation days.[7] Additionally, the expiry date is reduced by one day. If only five days to expiry are left, the time-to-expiry is set back to 35 days. The whole procedure is repeated 999 times, thus yielding 999×250 daily oRV estimates, each of which is computed from the successively refined intra-day resolution of the underlying asset price processes.

For simulation of the underlying price process in the BS model, we draw the appropriate number of normal innovations and compute the exact solution of the geometric Brownian motion. To keep an equal footing between the BS and Heston simulations, we use as BS (implied) volatility the square root of the Heston long-run variance from Table 5, i.e., $\sigma = \sqrt{0.0675} \approx 0.2598$. Option prices and the delta are calculated from the BS formulae.

For the Heston model, a Milstein scheme is employed for simulating the underlying asset. The parameters used are taken from the Heston model calibrated to option data from 2003-2011; see top panel of Table 5 and Section 4.3 for details on the calibration procedure. The variance process is started in the long-run variance level. Option prices are computed by direct integration of the characteristic function of the Heston model (Heston; 1993), and the delta and variance vega by two-sided finite difference quotients.

In theory, intra-day time decay as measured by theta should not impact oRV. In order to better understand the effect of the intra-day time decay on the estimates we run the

[7] Naturally, the artificial overnight return ensuing from the strike adjustment is not taken into account for estimating oRV, as is done in the empirical part.

described simulations twice: (*i*) all options are priced with a continuously adjusted time to expiry; (*ii*) we ignore intra-day time decay for option valuation, i.e., time to expiry of the option is adjusted only discretely by a whole day after each trading session.

3.4.2 Simulation results: BS model

The accuracy of the estimates is assessed by running OLS regressions of oRV on a constant and its underlying implied approximation dRV. Ideally, we would expect a zero intercept and a slope of one. Simulation results are presented in Tables 1 and 2 in terms of the 90% confidence intervals of the estimated coefficients that are obtained from the 999 runs.

TABLES 1 AND 2 ABOUT HERE

The left panel in Table 1 summarizes the results when correctly adjusting time to expiry intra-day. For the BS model, a small bias seems to be present. For neither intra-day frequency do the 90% quantiles of estimated intercepts and slopes comprise zero and one, respectively. In fact, the intercept is always estimated less than zero while the slope is larger than one. The bias, however, shrinks with decreasing sampling frequency. For the BS put, the average value drops from -0.0014 to -0.0003 for the intercept and for the slope from 1.0133 to 1.0024. The figures for BS call are very much akin. In addition, the width of the intervals shrinks substantially when choosing a smaller sampling frequency.

At this point, we can only conjecture where this bias stems from. Since we are using the exact solution to the geometric Brownian motion and the closed-form pricing formula, we expect the numerical noise to be relatively small. One possibility could be the presence of a finite sample gamma effect. The log-option price appears to be concave, which implies a negative gamma. As a consequence, the integral approximation may suffer from an omitted variables bias. Such an effect should be larger for options that are issued far away from at-the-money and closer when the option time-to-expiry is allowed to shrink to zero. Indeed, this expectation is confirmed by additional but unreported simulation results. The explanation also fits well with the results in the left panel in Table 2, which displays the same simulation results when intra-day time decay is (incorrectly) ignored.

In this case the bias is not removed but mitigated, since options cannot experience any intra-day time decay. The confidence intervals of the regression estimates now marginally contain the zero and the one; in addition, their width appears to be smaller.

3.4.3 Simulation results: Heston model

For the Heston model, simulation results show similar patterns. On average, the intercepts are negatively biased, whereas the slopes are positively biased. In general, the 90% confidence intervals are almost twice as large as for the BS case and do cover zero and one for the intercept and the slope, respectively. Shrinking the sampling frequency, leads to more accurate estimation results. The impact from ignoring intra-day time decay is the same as in the BS case.

Our reading of these results is that for the two-factor model, convergence occurs at a slower pace. Additionally, we expect convergence to be hampered by the larger numerical noise due to the various approximations involved in the Heston model. The differences between figures in Table 1 and 2 suggest that the same explanation for the observed bias would apply in the Heston case.

To gauge the effect of model misspecification, we also run the regressions for the Heston model, but assuming a BS model. An implied volatility compensated BS delta is used to replace the Heston delta while the additional contributions from stochastic volatility are ignored. Implied volatility is computed numerically by inverting the BS formula for each Heston option price. In this situation, the intercept is positively biased, but within the 90% confidence interval; the estimated slopes, however, are severely biased and range between 1.11 and 1.41 for the put and between 0.36 and 0.90 for the call. Decreasing sampling frequency or ignoring intra-day time decay has no visible impact on these sizable biases.

In unreported results, we redo these regressions for the Heston model, but now relying only on the Heston delta in the approximation of oRV. Contributions from stochastic volatility are ignored. In this case, slope estimates are biased in the same direction as in the case, when oRV in the Heston model is approximated by an implied volatility compensated BS delta, but the bias is even larger. Slope estimates range between 1.22 and 1.80 for the put and between 0.17 and 0.79 for the call.

4 Data

Our data set covers the time period from 01 July, 2003, to 8 November, 2011. It combines the intra-day index computations of the EURO STOXX 50® index; the EUREX traded intra-day transaction records of all futures (FESX) and options (OESX) having the EURO STOXX 50® index as underlying asset; interest rate data and (implied) dividend yields. We first describe the data sets and the data providers in general terms, report on the organization of data for the various empirical parts in this work, and comment on data filtering; specific details are deferred to the appendix.

4.1 Data description

Index data

EURO STOXX 50® index[8] was introduced in 1998 by STOXX Limited, Zürich, and is the leading financial market indicator in the Eurozone. It is a price index and comprises stocks of fifty EUR-dominated blue chips. Selection is based on free float market capitalization subject to a 10% weighting cap. As of 2012, the EURO STOXX 50® index captured close to 57% of the free float market capitalization represented by the Euro countries (Stoxx Limited; 2012). The index composition is reconsidered annually, whereas the weighting of index constituents is reviewed on a quarterly basis. Dividends that are paid out to stakeholders of the constituent stocks are not included in the index computation. Therefore, unlike performance indices that reinvest dividends, dividends need to be accounted for when valuing options written on this index. High-frequency data of the EURO STOXX 50® index starting as of 1 July, 2003 is available through Tick Data[9],

[8] ISIN = EU0009658145, Bloomberg code = SX5E, Reuters Instrument Code = STOXX50E.

[9] The homepage is www.tickdata.com

a subsidiary of Nexa Technologies, Inc., Irvine, CA. The time granulation for the index calculations between 9:00 and 17:30 CET is 15 seconds.

Futures and options data

The EUREX Frankfurt AG is a world-leading futures exchange, providing Euro-denominated benchmark derivatives that are widely recognized in terms of liquidity and cost efficiency. The most important equity products are the futures and options written on the EURO STOXX 50® index.

The futures contract (FESX) on the EURO STOXX 50® index is cash settled. It has delivery months in March, June, September and December. The last trading day is the third Friday in the expiry month, or if it is a bank holiday, the trading day prior to the third Friday.[10] The FESX has a contract value of EUR 10 per index point, and the minimum price change (or tick size) is one index point. Hence, one tick point corresponds to a price change of EUR 10 per contract. From 2003-2011, average daily open interest in the FESX futures rose from 1.3 to 2.7 million positions.[11]

Index options (OESX) are available as European style calls and puts on the EURO STOXX 50® index. The options are cash settled. Strike spacing is every 50 index points when a contract has up to 36 months to expiry, and 100 index points for longer-dated options. Expiry dates are the three nearest successive calendar months.[12] As for the FESX, expiry is the third Friday of each expiration month if this is an exchange day. Expiry dates of the futures contract and the options coincide in March, June, September and December. Price quotation in options is in points with one decimal; the minimum price change is 0.1 points, implying a tick value of EUR 1. Average daily open interest in the OESX options was around 9 million contracts in mid 2003 reaching about 45 million

[10]For further details on this and the rest of the discussion here, see, e.g., the quick guide on the FESX published by Eurex Frankfurt AG (2009).

[11]Source: Eurex Monthly Statistics.

[12]There are more expiry dates beyond the three nearest successive calendar months spanning up to 9 years and 11 months. However, this is not relevant to this work as only short dated options with up to three months to expiry provide sufficient liquidity.

contracts by the end of 2011 (aggregating open interest of both puts and calls).[13]

For academic use, the tick statistics of the FESX and OESX data can be received from the Karlsruher Kapitalmarktdatenbank[14] hosted at the Karlsruher Institute of Technology, Germany. Information provided is the trading day, a time stamp up to seconds, the expiry date, the strike and option type, a trading flag, the transaction price, quantity and total traded quantity.

Interest rates, implied dividend yields, and implied volatility

As risk-free interest rates we use the Euro Interbank Offered Rate (EURIBOR) from July 2003 to December 2007 and the Euro overnight index swap (OIS) rates from January 2008 to November 2011 (Source: Bloomberg, both series). We change the interest rate source in the sample, since by the end of 2007 the EURIBOR increasingly reflected credit risk of banks, which makes its use as a risk-free rate questionable. Interest rates are interpolated linearly to match the time-to-maturity of the futures and options data.

It is difficult to obtain information on expected dividends in the EURO STOXX 50® index. We therefore infer dividend yields from our knowledge of interest rate, options, futures and index data. Daily dividend yields are assumed to be constant intra-day and are implied for each given option time-to-expiry. For option expiries that coincide with a futures expiry, we exploit the forward valuation formula using intra-day futures prices and index levels to derive the dividend.[15] We take as an estimate the median of the dividend yields that are derived from all available futures-index pairs $(F_{t_i}^{t+\tau}, S_{t_i})$ available during day t. An admissible pair is defined by the closest possible consecutive observations between the index and the futures price, provided that no more than five seconds elapsed between them. For the remaining expiries we use the put-call parity. For each day we identify pairs of calls and puts of the same option series (unique strike and expiry date), for which the index was traded within a tolerance of 0.01%. Once more the median of

[13] Source: Eurex Monthly Statistics.

[14] fmi.fbv.uni-karlsruhe.de/149.php

[15] Using the forward valuation formula to price the futures contract is only approximate when rates are stochastic; but for the horizons relevant to this research (less than three months), it can be justified.

the dividend yields computed from the triple $(C_{t_i}, P_{t_i}, S_{t_i})$ is our estimate.

Given interest rates and dividend yields, implied volatility is backed out by equating the BS formula for calls and puts with observed market prices.

4.2 Data organization

From 2003-2011, the total raw option data set comprises approximately 5.8 million observations, 55% of which are puts and 45% calls. For our research, we organize this data in two ways. First, we create a set comprising the relevant time series of option data, index ticks and the futures prices. These data will be used to measure ex-post variation of options. Second, we create a data set which will be used for calibration of the Heston model. Our data filtering procedures are detailed in Appendix A.

Data set for estimation of option RV measures

For daily option RV computations, we identify for each trading day the most actively traded call and put option series, i.e., a specific combination of strike price and expiry date among all traded calls and puts of this particular day. We define 'most actively traded' in terms of transaction counts during the trading day. Note that we independently search for the most actively traded call and put; therefore the respective strikes, which are usually slightly out-of-the-money, but sometimes also the expiry dates, differ between calls and puts. Also, whereas the option series stays the same within the day, it necessarily differs from day to day. Typically, however, it is the same expiry date that is followed until roll-over close to expiry, while the strikes change depending on the drift of the index. Thus we do not follow the *same* strike price and *same* expiry date, as is done in the literature on option returns anomalies (Coval and Shumway; 2001; Jones; 2006; Broadie et al.; 2009). Cum grano salis, the moneyness characteristics of the options, however, stay similar over the entire sample period from 2003–2011, as the options identified by our procedure are those close to at-the-money; see Figure 1. In the top panel the EURO STOXX 50® is shown along with selected strikes. The bottom panel plots the moneyness of the options selected. It seems that at the climax of the financial crisis the most heavily traded options are somewhat deeper out-of-the-money than in calmer periods. Further details on these data (after filtering) are summarized in Table 3.

FIGURE 1 AND TABLE 3 ABOUT HERE

After daily puts and calls have been identified, the most recently known level of the underlying asset is assigned to each observation, i.e., the index level and the last traded futures prices stemming from the most actively traded expiry. These values will be used for computing the realized measures.

We point out that for estimating the realized measures, we do *not* make use of all available ticks. It is well known that in the presence of market micro structure noise, overly frequent sampling will result in biased RV estimates (Bandi and Russel; 2006; Hansen and Lunde; 2006). A conventional way to mitigate these effects when using the classical RV estimators as in Section 3 is to sample at a lower frequency than potentially possible. Suggestions for the sampling frequency range between five and sixty minutes depending on the liquidity of the asset (Andersen et al.; 2000; Andersen, Bollerslev, Diebold and Ebens; 2001; de Pooter et al.; 2008; Patton; 2011). Given this empirical evidence, we adopt a tick time sampling of about 30 (20, 10) minutes on average. By tick time sampling we refer to sampling ticks such that each tick is (on average) 30 (20 or 10) minutes apart. For the thirty minutes frequency this results in roughly 19 observations per day used for estimating oRV. The tick sampling frequency depends on the number of observations available at the respective day; see Dacorogna et al. (2001) and Hansen and Lunde (2006) for a thorough discussions of tick time sampling and other sampling schemes for high-frequency data.

Calibration data set

Since calibration of an option pricing model requires a cross-section of traded calls and puts with different strikes and, if possible, expiry dates, this data set comprises, day by day, all available strikes and expiry dates, both from calls and puts. Since calibration will be based on the index only, each observation is combined with the most recently observed index level. The actual calibration of model parameters is carried out only on a subset of all observations, namely on Wednesdays; see Section 4.3 for further details. This choice mitigates expiry effects and substantially reduces the computational burden involved; see e.g. Bates (1996), Christoffersen and Jacobs (2004) or Gruber et al. (2010) for details of this practice. The extraction of the latent factor is eventually done on all days available; for descriptive details on the calibration data set after filtering, see Table 4. In Figure 2, top panel, we present the at-the-money implied volatility levels and the implied volatility skews measured in the calibration data set for the time period from 2003 to 2011.

FIGURE 2 AND TABLE 4 ABOUT HERE

4.3 Intra-day calibration of the Heston model

Calibration of an option pricing model such as the Heston model requires both estimation of the model's structural parameters $\boldsymbol{\theta} = (\kappa, \lambda, \xi, \rho)^\top$ and the series of latent spot volatilities $\{V\}_t$. A number of different estimation and filtering techniques have been suggested to this end.[16] In this study, we follow the two step-procedure suggested in Bates (2000). We slightly modify the procedure to make it applicable to intra-day data; see also Huang and Wu (2004), Christoffersen et al. (2009), and Gruber et al. (2010) for applications of D. Bates' procedure.

For identification of the volatility process at each point in time, a sufficiently densely populated cross-section of options is required; otherwise the estimation process degenerates. In working with intra-day transaction data, this is a challenge, since option trades occur at random times. Hence, we cannot estimate the intra-day volatility process in a continuous fashion. We therefore assume that the Heston volatility process is piecewise constant

[16]See, e.g. Bakshi et al. (1997), Eraker (2004), Broadie et al. (2007), and Carr and Wu (2007), among others.

on $J = 8$ intra-day subintervals. Since each day has 8.5 hours of trading, each subinterval is slightly larger than one hour.[17] In this way, we include all option observations available on date t within the jth subinterval to estimate an average realization of the volatility process on this subinterval that will be denoted by $\hat{V}_{t,j}$.

We base calibration on the cost functional

$$\begin{aligned} \mathcal{K}(\boldsymbol{\theta}, \{V\}_{t,j}^{T,J}) &= \frac{1}{TJ} \sum_{t=1}^{T} \sum_{j=1}^{J} \mathcal{K}_{t,j}(\boldsymbol{\theta}, V_{t,j}) \\ \mathcal{K}_{t,j}(\boldsymbol{\theta}, V_{t,j}) &= \frac{1}{N_{t,j}} \sum_{k=1}^{K_{t,j}} \sum_{i=1}^{N_{t,j,k}} w_{t,j,k,i} \left(H_{t,j,k,i} - H_{t,j,k,i}(\boldsymbol{\theta}, V_{t,j}) \right)^2 \end{aligned} \tag{27}$$

where $N_{t,j,k}$ is the number of all options traded in day t and intra-day interval j having time to maturity T_k, where $k = 1, \ldots, K_{t,j}$. The total sum of options traded in day t and intra-day interval j is $N_{t,j} = \sum_{k=1}^{K_{t,j}} N_{t,j,k}$. By $H_{t,j,k,i}$ we denote observed prices and by $H_{t,j,k,i}(\boldsymbol{\theta}, V_{t,j})$ Heston model prices with parameter vector $\boldsymbol{\theta}$. The cost functional overweights the short-dated options that are of particular interest to the study. This is achieved by using piecewise constant weights $w_{t,j,k,i}$ that overweight options with a time-to-expiry less than 30 days by a factor two.

The calibration procedure is iterative in nature and encompasses the following two steps until only minor changes occur:

1. Given an initialization of the latent factor, find

$$\hat{\boldsymbol{\theta}} = \arg\min_{\boldsymbol{\theta}} \quad \mathcal{K}(\boldsymbol{\theta}, \{V\}_{t,j}^{T,J}) \; .$$

2. With a working estimate $\hat{\boldsymbol{\theta}}$, solve the optimization problems

$$\hat{V}_{t,j} = \arg\min_{V} \quad \mathcal{K}_{t,j}(\boldsymbol{\theta}, V_{t,j}) \qquad t = 1, \ldots, T, \; j = 1, \ldots, J \; .$$

[17] We also experimented with shorter subintervals. This works in principle since only a single option is required to (exactly) determine $\hat{V}_{t,j}$. Shorter subintervals, however, lead to a more erratic estimated volatility process, and in consequence to more noise in the estimated Heston greeks. Another issue is the dramatically increasing computation time. These considerations led us to choose the outlined strategy.

A serious threat to evaluating the cost functional (27) is that it is computationally inefficient in an intra-day setting where each option $H_{t,j,k,i}$ is observed at a different spot price. The direct integration approach used in the simulation exercise presented in Section 3.4, where emphasis is put on accurately computing greeks, is not feasible for the calibration problem. Ideally we would like to price *all* options with fixed expiry date within each subinterval by a single evaluation of a fast Fourier transform (FFT) pricer which returns an entire set of option prices on a strike grid, such as the FFT pricer by Carr and Madan (1999). However, with the underlying asset price fluctuating *within* each subinterval, this is impossible.

We resolve this issue by exploiting a homogeneity property. Denote by $H(X, S, T)$ an option price with strike X, underlying asset price S, and expiry data T. If the underlying asset price dynamics is independent from the unit of measurement, it holds that $H(X, S, T) = \alpha^{-1} H(\alpha X, \alpha S, T)$ since H is homogeneous of degree one in X and S. For the Heston model this property holds.

Denote by $H_{t,j,k,i}(X_i, S_i, T_k) = H_{t,j,k,i}$, $i = 1, \ldots, N_{t,j}$ a subsample of observed option prices with fixed expiry date T_k which is realized in the jth subsample on date t. From the preceding discussion it is then clear that rather than pricing each option separately, we can price all options in subsample j by using a single evaluation of the FFT-pricer on the modified Heston prices $\alpha_{ji}^{-1} H_{t,j,k,i}(\alpha_{ji} X_i, \bar{S}_j, T_k; \boldsymbol{\theta}, V_{t,j})$, where $\alpha_{ji} = \bar{S}_j / S_i$ and $\bar{S}_j$ denotes the mean spot price in subinterval j. This homogeneity trick substantially alleviates the computational burden involved, since we are able to price all options within each interval j by $K_{t,j}$ price evaluations, i.e., the number of observed expiry dates in each interval.

The calibration results on the whole 2003-2011 sample and on the pre-crisis subsample 2003-2007 are summarized in Table 5. These results are obtained by holding the level of mean reversion fixed at $\kappa = 2.0$. We fix κ, since in the Cox-Ingersoll-Ross process the unconditional variance is given by $\lambda\xi^2/(2\kappa)$. Thus, at a given level of mean reversion λ and unconditional variance, large values in ξ incite large values in κ and vice versa (Jiang and Knight; 2002, p. 208). This property may slow down or impede calibration. The selected level $\kappa = 2.0$ is close to the values typically reported for broad equity indices and also suggested in Bergomi (2004). Finally, we carry out the calibration in imposing the Feller condition $2\lambda\kappa \geq \xi^2$, which ensures a strictly positive solution for the Cox-Ingersoll-Ross process.

FIGURE 2 AND TABLE 5 ABOUT HERE

In Figure 2, lower panel, we display the RV series of the underlying that is implied from calibrating the Heston model. Up to an annualization factor, this series is given by summing the estimates of $\hat{V}_{t,j}$, i.e. $RV_H(t) = \sum_{j=1}^{J} \hat{V}_{t,j}$. We contrast this estimate with the RV series of the index estimated using (18) on five minute returns. The correspondence between the two series is by no means perfect, but it is obvious that intra-day option trades capture the RV dynamics of the underlying to a large extent.

5 Tests of model predictions

We present here the results of the tests of the model predictions introduced in Section 2.4. We verify the goodness-of-fit along several dimensions: graphical inspection of the option RV series (observed and underlying-based) and of their differences, analysis of the unconditional cumulative distribution functions, and pairwise regressions.

5.1 Option realized volatility series

As an illustrative starting point, we show the daily time series of oRV obtained from high-frequency transactions in puts and calls in Figure 3. The plot additionally features dRV using the BS approximation for the underlying index.

FIGURE 3 ABOUT HERE

First, it is important to highlight that the time series dynamics of oRV differs strongly from what is usually observed for the realized variances of indices or other delta-one instruments; see for comparison purposes the RV series of the underlying index plotted in

Figure 2. Series of oRV are more rapidly fluctuating and less autocorrelated and do not display a long memory feature. Clearly, this stylized fact might be a consequence of the "roll-over strategy" needed to compute RV for options and of the fact that for each day we take options with different strikes (most liquid options); for details, see the discussion in Section 4.2 or Figure 1.

If we compare the two series in Figure 3, we find the approximation based on the BS model for the underlying index to be reasonable at first sight. It closely follows the oRV computed from high frequency data in the option market. For further investigation, we therefore display the differences among the series in Figure 4.

FIGURE 4 ABOUT HERE

Let us first focus on the top panel obtained from the one-factor BS model. Differences among the series can be very pronounced for some periods and are clearly not negligible. This is a first warning about the accuracy and the reasonableness of the BS approximation for the underlying index. Starting with 2007 and during the whole financial crisis there is a clear tendency of BS-based dRV to be systematically larger (smaller) than the one observed on the option market for call (put) options. In particular, the average value of the differences is two times larger for the 2007-2011 period than for the period before (2003-2006) for put options (-0.035 vs. -0.018, respectively). This loss in accuracy of the dRV is even more evident for call options: after the beginning of the financial crisis, differences have become on average four times larger than before (0.054 vs. 0.015).

These results may be a consequence of the rigid structure imposed by the BS model, which is not able to react to changing market conditions. Comparing Figure 2, top panel, and Figure 4, it seems that the deterioration of the approximation quality coincides with the steeper implied volatility skew. Indeed, this is consistent and to be expected given the theoretical discussion in Section 2.3. Since the simple BS-Delta does not take into account the implied volatility dynamics, it might perform well in calm and trending markets. During and after the financial crisis (2007-2011 period), with rising uncertainty (compare the index levels shown in Figure 1 with implied volatility levels and the implied volatility skew in Figure 2), this correction term may gain importance, which explains the impairment of the approximation quality.

Are these differences still present when using the more flexible stochastic volatility approximation for the underlying index, such as the Heston model? Results are shown in the bottom panel of Figure 4. As shown in the figure, differences are still visible. Allowing for stochastic volatility does not seem to be able to eliminate the mismatch between the two series, although during the financial crisis differences are less evident and striking (-0.024 and 0.026 for put and call options, respectively). Surprisingly, there seems to be a clear bias in the 2003-2006 period. Under stable market conditions, i.e., low volatility and uncertainty in the spot market, there is more variability in call options than predicted by the Heston-based approximation (the contrary is true for put options). This behavior may once again be reconciled with the previous explanation based on the implied volatility skew, since for the Heston model property (17) holds. To a certain degree, it can therefore accommodate changes in implied volatility dynamics that are related to the implied volatility skew. It seems, however, the Heston model over-compensates in the non-crisis period.[18]

In summary, this section provided initial evidence that neither the BS model nor the Heston model for the underlying dynamics may be suitable for capturing the second-order moments observed in the options market. The higher degree of flexibility allowed by introducing stochastic volatility does not seem to be sufficient to produce option realized variances consistent with the observed ones.

5.2 Option realized volatility cumulative distribution functions

Figure 5 shows the cumulative distribution functions (CDF) of oRV and those of the BS-based dRV. The red dotted lines indicate the 95% confidence interval for the empirical CDFs based on Greenwood's formula. The BS-based dRV introduced in equation (20)

[18] In fact, when calibrating to the non-crisis period, we obtain a smaller correlation coefficient which implies an implied volatility skew that is shallower; see Table 5. Then differences become smaller, but are still visible.

are computed using the different approximation schemes introduced in Section 3.2: t and $t-1$ denotes the times when evaluation of $\tilde{\Delta}$ is done: t is at the beginning of the return interval (Ito discretization) and $t-1$ at the end; "over" and "under" denote the minimal and maximal weighting factors which yield bounds for the whole integral term.

FIGURE 5 ABOUT HERE

As a first insight from Figure 5, all four BS-based approximations to option RV yield very similar results: all CDFs are very close and exhibit almost no differences. Thus, we discuss results only with respect to the computation based on $t-1$, i.e., the Ito discretization.

In the top panel, results for the call options are presented. There are huge differences between the CDFs when comparing oRV and BS-based dRV. At all quantile levels, the BS-based dRV is systematically larger than what is directly observed from options, supporting the results found in the last section. In some sense, one may interpret Figure 5 as exhibiting "first-order stochastic dominance" of call options RV. This unusual interpretation is due to the fact that CDFs of second-order moments are considered and is meant in the sense that BS-implied call dRV considerably overestimates risk (at least the one captured by second-order moments) at all quantile levels. Turning to puts (see bottom panel of Figure 5), we likewise discern smaller but significant differences between the CDFs. Consistent with our previous results, BS-implied put dRV systematically underestimates the risk observed in the options market.

Remarkably, these results could be compatible with oRV if a stochastic volatility factor is missing. Following (15), oRV splits into three contributions I_1, I_2 and I_3, the last of which changes sign between calls and puts. Thus, if I_3 outweighs I_2 in terms of size, an estimate based on I_1 alone would systematically overestimate (underestimate) calls oRV (puts oRV) and patterns such as observed in Figure 5 could arise.

We therefore now turn to the results for the CDFs when considering the two-factor Heston model for the underlying index. In Figure 6, four CDFs are reported: (*i*) for the oRV (solid black lines, together with dotted lines for the 95% confidence bounds); (*ii*) the full Heston-based dRV using the derivation given in (15), which includes all three integral terms estimated according to (20), (21) and (22) (dotted-dashed lines); (*iii*) the Heston-based dRV using solely (20), similarly to the BS case (dotted lines); and (*iv*), for comparison purposes, the BS-based dRV CDFs (solid, grey lines).

FIGURE 6 ABOUT HERE

Let us start with the call option results shown in the top panel. The benefits from allowing for stochastic volatility are clearly visible: adding this second factor in the underlying dynamics is able to partially close the mismatch between the observed and Heston-based CDFs. Nevertheless, the gap between the two functions is still present, in particular for very small and very high quantiles. In contrast to the BS case, the curves no longer display the reverted first-order stochastic dominance structure. It seems that in using the Heston model for the underlying dynamics, the RV is underestimated at low quantiles, whereas large values of RV are marginally, but still significantly, overestimated. Once again this result is in line with the discussions in the previous section. Adding stochastic volatility is a step in the right direction, but is conceivably not sufficient to produce call option second-order moments that are consistent with the observed ones.

In the bottom panel of Figure 6, the same CDFs obtained for puts are plotted. The huge discrepancy that was obtained with BS-based dRV has vanished. There is essentially no difference between Heston-implied and oRV CDFs. Stochastic volatility seems to work extremely well in this case. Thus, the Heston model seems to be consistent with observed put realized volatilities, at least based on the graphical inspection of the unconditional CDFs. In the next section, we show that this is not completely true when considering pairwise regressions of observed realized volatilities on Heston-based realized volatilities.

Finally, we evaluate the effect of stochastic volatility for options second-order moments in the Heston setting. In Figure 6 the difference between the dRV CDFs obtained using the whole sum of the three terms in (15) and neglecting the two additional terms due to stochastic volatility is a priori hardly imaginable (dotted-dashed line vs. dotted line). The contribution of stochastic volatility for the final accuracy of the option realized volatilities is substantial. Neglecting the two additional terms would lead to realized volatilities that are even less accurate than those obtained using the BS approximation. By and large, this corresponds with our findings in the simulations; see Section 3.4.

In Figure 7, we try to quantify the contribution of stochastic volatility in the following way: We report the ratio between I_1 and $2I_3$. This third term has opposite signs for put and call options and depends on the product of the two greeks $\tilde{\Delta}$ and $\tilde{\nu}$. The contribution of the second term to the whole sum is smaller and therefore not reported.

FIGURE 7 ABOUT HERE

The results confirm that the contribution of stochastic volatility may be substantial depending on the time period. Interestingly, it appears that during the financial crisis the relevance of the additional third factor diminishes. This finding is attributable to two factors. First, it might be a consequence of sampled option prices. Between 2008-2009, the moneyness of the most liquid options under investigation is changing (see again Figure 1) as deeper out-of-the-money options are traded. Since in general these options have a smaller vega, the third factor is lower in magnitude and odds may shift in favor of the first factor. Second, recent studies of realized variances in index and futures markets have shown that during the financial crisis, simple locally constant volatility models yield very accurate RV predictions and are difficult to beat by more flexible approaches; see, among others, Audrino and Knaus (2012). This fact would also explain the dominance of I_1.

Summarizing, adding stochastic volatility as a second factor in the underlying dynamics improves the fit and makes derived option second-order moments closer to the observed ones.

5.3 Option realized volatility regressions

Similarly to the simulation part in Section 3.4, we report here the results obtained when regressing oRV on a constant and on the BS- or Heston-based dRV. If the regressions yield constants not significantly different from zero and slope coefficients not significantly different from one (or at least biases of comparable size), we may conclude that the model approximations for the underlying index dynamics cannot be rejected by the data.

Results for the regressions are reported in Tables 6 and 7 for put and call options, respectively. To account for possible autocorrelations and heteroscedasticity, standard errors are computed using Newey-West estimators.[19] Results are reported for different moneyness m and time-to-maturity τ ranges. In the different panels of the tables, from top to bottom we enlarge the moneyness range to be included by $1 - m_i \leq m \leq 1 + m_i$, thus allowing for more heterogeneity in the moneyness dimension; from left to right, we successively exclude options with low time-to-maturity, i.e., $\tau < \tau_k$.

TABLES 6 AND 7 ABOUT HERE

First, for both put and call options we always find a small, statistically significant intercept. The estimate is at least ten times larger than the one found in the simulations, and – in sharp contrast to the simulations – always positive. This estimated intercept indicates a global shift in the level of oRV. There are several possible reasons for this result: (i) this large positive shift may be a global moneyness effect given that the options we consider have more heterogeneous strikes than in the simulations[20]; (ii) and alternatively, the shift may be due to differences in the microstructure noise between the two markets. While the options are traded within a bid-ask spread, the underlying index is continuously calculated from its fifty constituents, which is likely to average out the effect of the bid-ask bounce.

Second, in line with previous evidence, the BS-approximation generally overestimates (underestimates) the RV for call (put) options. The deviations of the estimated slope coefficients are in the same direction, but smaller than our simulation results would suggest when using solely the BS-based dRV approximation in a pure Heston model; compare the right-most panel in Tables 1 and 2. In contrast, the Heston-based dRV tends to be too

[19]The number of lags used is determined by $4(\frac{n}{100})^{1/4}$, floored to the nearest integer; n is sample size.

[20]As supporting empirical evidence for this explanation, we run similar regressions including moneyness as an additional predictor. We saw that the intercept and the moneyness factor are highly correlated and have similar regression coefficients with different signs. For this reason we exclude the intercept in the regressions of Section 6.1.

large for both call and put options. The slope coefficients are in general significantly smaller than one and far beyond those we obtained in the simulations. Note that this result is true (though less evident) for put options as well, showing that the impression we derived from the visual inspection of the CDFs of the accuracy of the Heston-based approximation for put options may be misleading.

Across different moneyness and time-to-maturity filters, all regressions yield qualitatively the same picture, but it appears that both BS- and Heston-based approximations gradually deteriorate when excluding short-dated options and/or enlarging the moneyness range. This suggests that both model approximations do not correctly capture the variation in oRV across the various expiry dates.

Finally, when comparing BS and Heston results, we can conclude that in general allowing for stochastic volatility improves on the accuracy of the derived option realized volatilities. However, neither the BS model nor the Heston model is able to fully capture the second-order moments observed in the option market. Also, there seems to be a wedge between both markets. While the model-based approximations do not seem to do badly for puts, the approximations are particularly poor for calls. For both models, observed call oRV are significantly smaller than both models would suggest.

6 Further results

In this section, we test the robustness of the results found in the last section along several dimensions. First, we extend the discussion to additional factors which might impact oRV. Second, we test the stability of the results. More specifically, we test (*i*) along different sampling frequencies on which we compute oRV; (*ii*) on a time period excluding the recent financial crisis; (*iii*) we use a potentially more robust estimator based on mean-variance principles; and (*iv*) we exclude days with a high number of a certain type of observational violations of option and underlying price movements in the spirit of Bakshi et al. (2000a).

6.1 Additional factors

We extend the regression results shown in Section 5.3 by including additional predictors. Given the relative stability of the regressions with respect to different moneyness and time-to-maturity filters, we report only the results for options with expiry larger than 5 days and moneyness in the range $[0.9; 1.1]$.

As additional factors we consider:

- moneyness (m) and time-to-maturity (τ) to capture systematic cross-sectional heterogeneity which may have an impact on oRV. Given the high correlation between the intercept and m, we exclude the intercept in these regressions.

- We estimate the underlying's RV using the classical estimator in (18) based on five-minute returns. The aim is to verify whether we can still capture stochastic volatility components that are not modeled by the three-factor composition estimated from the Heston model alone.

- Following the evidence presented for example in Han (2008), we introduce a dummy for high/low uncertainty in the market. As a proxy for uncertainty we use similarly to Han (2008) the underlying index volatility measured by values of RV larger or smaller than 0.01; see Figure 2. The aim is to see whether the regression results (in particular the significance of the slope coefficient for dRV) change for different market conditions.[21]

Results of the additional regressions are shown in Tables 8 and 9. Standard errors are computed using Newey-West estimators to correct for possible autocorrelations and heteroscedasticity.

TABLES 8 AND 9 ABOUT HERE

Let us first discuss the results of the regressions without the underlying's volatility dummy.

[21]We also used other similar dummy variables, for example for up and down movements of the underlying index. Results were qualitatively the same and may be obtained from the authors upon request.

As expected, including moneyness has a marginal impact in the regressions: moneyness takes the role of the constant term in the previous regressions (recall that moneyness is always in the neighborhood of one). The effect of time-to maturity is significantly negative in all cases, whether for BS or the Heston-based approximations. The larger time-to-maturity, the more the model-based approximations overpredict oRV. Adding the underlying's RV to the regressors has an effect only on put oRV. The underlying's RV significantly increases the option oRV. For calls the sign is negative but insignificant. This finding suggests that there are additional stochastic volatility components which are not correctly captured by the Heston model and which act on oRV in the sense of the sign-switching term I_3. As a final remark, note that the BS and Heston dRV slope coefficients are hardly influenced by the inclusion of all these factors and remain fairly unchanged.

Consider now the regression results when explicitly taking market uncertainty into account. Several results are worth highlighting. First, for both put and call options in the Heston setting, the underlying's RV has a significant effect on oRV during periods of low and stable market conditions, whereas it has no (or much smaller) effect in times of market distress. It acts in opposite directions: it tends to increase (decrease) oRV for put (call) options.

Second, for put options the BS-based dRV is adequate for the low volatility regime and is only marginally rejected during periods of high market uncertainty. The Heston-approximation cannot be rejected for periods of high market uncertainty but fails (dRV is too high) in the other regime. Third, for call options the BS approximation yields options second-order moments that are too large compared to the observed ones. This result is true for both regimes but most evident for the high volatility regime. The additional flexibility allowed by the Heston model yields an improvement in accuracy, in particular in periods of low market volatility. These findings are in line with those presented in Han (2008) and may be seen as a confirmation that probably an important factor relevant to option pricing is missing in the models under consideration.

6.2 Robustness checks

6.2.1 Other frequencies

Hare we check in which way changing the tick sampling frequency of 30 minutes for the computation of oRV affects the results presented in Section 5. Similarly to the simulations, we redo the analysis using option prices on 10 and 20 minute intervals. Results are very close to the ones we presented in the previous sections and therefore not reported. All discussions and conclusions also still hold when considering other frequencies.

6.2.2 No financial crisis

We redo the whole analysis only on the pre-crisis period to see whether our findings are driven by the financial crisis. To this end we only use the pre-crisis sample from 2003 to 2007. For the sake of brevity, we report results only for the regressions. They are summarized in Tables 10 and 11.

TABLES 10 AND 11 ABOUT HERE

Results are qualitatively similar to the ones we discussed in Section 5.3. It seems, however, that in the pre-crisis period the approximation quality for calls is slightly improved. All in all, however, we do not find that results could be specifically attributed to the financial crisis. They appear to be stable over different sub-periods and market conditions.

6.2.3 Mean-variance approach

The present analysis could be challenged on the grounds that the figures obtained for the Heston model might be harder to estimate since three integral terms need to be obtained. This could lead to larger estimation noise and thus to less accurate estimates. Moreover, the estimates $\hat{I}_2$ and $\hat{I}_3$ also depend on the filtered Heston latent variance, which introduces additional model dependence. To investigate this issue, we study the performance of a minimum variance (MV) delta.

The MV delta is a delta than minimizes the instantaneous variance of a purely delta-hedged portfolio.[22] It is given by

$$\Delta^{mv} = \Delta_C + \nu \frac{d[S,V]}{d[V]} \ ,$$

where Δ denotes the usual (call) delta and ν the variance vega. By the covariation in the numerator, the second term depends on correlation. Therefore it is zero whenever the Brownian motions driving the two-factor model are uncorrelated. Since for equity markets correlation is typically negative, the MV call delta leads to an underhedge relative to the usual model call delta. For the Heston model, the formula specializes to

$$\Delta^{Hmv} = \Delta_C^H + \frac{\rho\xi}{S}\nu \ .$$

In the analysis with the MV delta, we may treat the stochastic volatility as a one-factor model and consider only an estimate for I_1. Similarly as in Section 3.2 we define weighted returns

$$\tilde{r}_{j,t} = \tilde{\Delta}_C^{Hmv}\Big[y\Big(t-1+\frac{j}{M}\Big) - y\Big(t-1+\frac{j-1}{M}\Big)\Big], \ j=1,\ldots,M,$$

where $\tilde{\Delta}_C^{Hmv} = \Delta_C^{Hmv}\frac{S}{C}$ (with the understanding that evaluation of this term takes place at the beginning of the time interval as discussed in Section 3.2). Then

$$dRV_{\tilde{y}_1}(t) = \hat{I}_1^{mv} = \sum_{j=1}^{M} \tilde{r}_{j,t}^2 \approx \int_{t-1}^{t} (\tilde{\Delta}_C^{mv})^2 \ \sigma^2(u)du \ . \qquad (28)$$

If the three separate estimates of the integral terms are of similar quality as a single one, we would expect that $\hat{I}_1^{mv}$ performs like $\hat{I}_1 + \hat{I}_2 + 2\hat{I}_3$.

In our simulations and empirical analysis, we indeed find this to be the case. In fact, using the single-term approximation based on the MV delta rather than the triple sum of separate terms yields close to indistinguishable results. We therefore do not report them. We take this as evidence that the results for the Heston model using $\hat{I}_1 + \hat{I}_2 + 2\hat{I}_3$ are not driven by spurious noise.

[22]The MV delta has been extensively studied in Bakshi et al. (1997), Bakshi et al. (2000b), Alexander and Nogueira (2007) among others.

6.2.4 Excluding violations

Based on a taxonomy presented in Bakshi et al. (2000a), we test whether our findings are particularly affected by days when the number of intra-day underlying movements and option prices is not in accordance with properties shared by all one-dimensional diffusion option models. Let us denote with ΔS (ΔC or ΔP) the intra-day changes of the underlying index price (call or put price, respectively). Bakshi et al. (2000a) define four types of violations, the second and third of which appear to be the most relevant for our analysis:

(II) $\Delta S \neq 0$ but $\Delta C = 0$ for call options and $\Delta P = 0$ for put options.

(III) $\Delta S = 0$ but $\Delta C \neq 0$ for call options and $\Delta P \neq 0$ for put options.

Our results may be particularly sensitive to days with a large fraction of violations of type II or III above, given that they are based on comparisons of the realized volatilities. This is because for computing RV of the index and the options we consider sums of intra-day changes. The time series of the proportions of these two types of violations is plotted in Figure 8.

FIGURE 8 ABOUT HERE

Depending on the time period, the proportion of intra-day violations may be quite substantial for type II errors, totaling as large as 30-40% of the total number of intra-day changes. This can be understood by noting that small changes in the index, which is continuously calculated up to two digits, are not sufficiently large to trigger revisions in option prices that are quoted within a bid-ask spread. In contrast, type III errors are negligible.

We redo the regression analysis excluding days with more than one occurrence of type II violations, but ignore type III violations given their irrelevance; see Tables 12 and 13.

TABLE 12 AND 13 ABOUT HERE

As to be expected, the results of the different tests of the BS-model predictions improve for both puts and calls. Across all moneyness and time-to-maturity filters, it is difficult to reject the hypothesis that the slope coefficient is equal to one for puts oRV when considering Heston-based dRV. By contrast, the BS-based approximation is uniformly rejected. For call oRV the changes are tiny. The strict segregation in the approximation quality between put and call oRV, however, continues to hold.

7 Concluding remarks

We presented an empirical investigation of whether classical one-dimensional and two-dimensional diffusion processes are able to reproduce ex-post intra-day variability observed in option prices. Thanks to the availability of high-frequency data, accurate measures for the unobservable option second-order moments can be obtained: realized variances. Our analysis is based on the differences among option realized variances and model-based approximations of realized variances obtained from the Black and Scholes and Heston models. We showed that these widely used benchmark models are not consistent with what is observed in second-order moments in the option market. Our analysis thus adds an intra-day perspective to the existing literature studying the performance of these models on lower frequencies, such as daily or weekly data.

The present analysis could be refined and extended in many directions. First, the Heston model is very restrictive. In fact, it could even be too limited to capture the salient features of short-dated at-the-money options and their associated volatility dynamics, as required by our study. Recent research by Christoffersen et al. (2010) suggests that non-affine stochastic volatility models, such as Jones (2003) or Aït-Sahalia and Kimmel (2007) may substantially improve on these deficiencies. Second, one could allow for richer volatility dynamics, for instance by modeling stochastic leverage. In fact, Christoffersen et al. (2009) provide evidence that allowing for a transitory and a permanent component in the volatility process cuts option pricing errors both in- and out-of-sample; see also Gouriéroux et al. (2009) and Gruber et al. (2010) for related multi-factor stochastic volatility models. Third, ample empirical evidence underscores the relevance of jumps for modeling equity return data and pricing equity options; see Bakshi et al. (1997), Pan (2002), Eraker (2004), Bollerslev and Todorov (2011), among others. While the inclusion of more stochastic volatility factors and jumps is likely to render the estimation of the additional contributions to option realized variance considerably more intricate, it seems natural to expect that these extensions potentially close the observed gaps between option realized variance and its model-based approximations. Finally, our results appear to indicate that some relevant factors influencing the underlying and/or option price processes are still missing. In fact, recent research on option prices has shown that purely rational models such as the ones we considered in our investigation, are not able to completely reconcile model-based option prices with observed option prices; see, among others, Poteshman (2001) and Han (2008). There it has been found that including behavioral factors to explain option prices significantly improves the fit. We leave these topics for further research.

References

Aït-Sahalia, Y. and Kimmel, R. (2007). Maximum likelihood estimation of stochastic volatility models, *Journal of Financial Economics* **83**: 413–452.

Alexander, C. and Nogueira, L. M. (2007). Model-free hedge ratios and scale-invariant models, *Journal of Banking and Finance* **31**(6): 1839–1861.

Andersen, T. G., Bollerslev, T. and Diebold, F. (2010). Parametric and nonparametric measurement of volatility, *in* Y. Aït-Sahalia and L. Hansen (eds), *Handbook of Financial Econometrics*, Vol. 1, North Holland, Amsterdam, pp. 67–137.

Andersen, T. G., Bollerslev, T., Diebold, F. X. and Ebens, H. (2001). The distribution of realized stock return volatility, *Journal of Financial Economics* **61**: 43–76.

Andersen, T. G., Bollerslev, T., Diebold, F. X. and Labys, P. (2000). Great realizations, *RISK* **13**: 105–108.

Andersen, T. G., Bollerslev, T., Diebold, F. X. and Labys, P. (2001). The distribution of realized exchange rate volatility, *Journal of the American Statistical Association* **96**: 42–55.

Andersen, T. G., Bollerslev, T., Diebold, F. X. and Labys, P. (2003). Modelling and forecasting realized volatility, *Econometrica* **71**: 579–625.

Andersen, T. G., Fusari, N. and Todorov, V. (2012). Parametric inference and dynamic state recovery from option panels, *Working Paper 18046*, National Bureau of Economic Research.

Audrino, F. and Knaus, S. (2012). Lassoing the HAR model: A model selection perspective on realized volatility dynamics, *Technical report*, St. Gallen University.

Bakshi, G., Cao, C. and Chen, Z. (1997). Empirical performance of alternative option pricing models, *Journal of Finance* **52**(5): 2003–2049.

Bakshi, G., Cao, C. and Chen, Z. (2000a). Do call and underlying prices always move in the same direction?, *Review of Financial Studies* **13**(3): 549–584.

Bakshi, G., Cao, C. and Chen, Z. (2000b). Pricing and hedging long-term options, *Journal of Econometrics* **94**: 277–318.

Bakshi, G., Madan, D. and Panayotov, G. (2010). Returns of claims on the upside and the viability of U-shaped pricing kernels, *Journal of Financial Economics* **97**: 130–154.

Bandi, F. M. and Russel, J. R. (2006). Separating microstructure noise from volatility, *Journal of Financial Economics* **79**(3): 655–692.

Barndorff-Nielsen, O. E., Hansen, P. R., L. A. and Shepard, N. (2009). Realised kernels in practice: trades and quotes, *Econometrics Journal* **12**(3): C1–C32.

Barndorff-Nielsen, O. E. and Shepard, N. (2001a). Econometric analysis of realised volatility and its use in estimating stochastic volatility models, *Journal of the Royal Statistical Society B* **64**: 253–280.

Barndorff-Nielsen, O. E. and Shepard, N. (2001b). Non-Gaussian Ornstein-Uhlenbeck-models and some of their uses in financial economics, *Journal of the Royal Statistical Society B* **63**: 167–241.

Barndorff-Nielsen, O. E. and Shepard, N. (2002). Estimating quadratic variation using realized variance, *Journal of Applied Econometrics* **17**: 457–477.

Barndorff-Nielsen, O. E. and Shepard, N. (2004). Power and bipower variation with stochastic volatility and jumps, *Journal of Financial Econometrics* **2**(1): 1–37.

Bates, D. S. (1996). Dollar jump fears, 1984:1992, distributional anomalies implicit in currency futures options, *Journal of International Money and Finance* **15**: 65–93.

Bates, D. S. (2000). Post-'87 crash fears in the S&P 500 futures option market, *Journal of Econometrics* **94**: 181–238.

Bates, D. S. (2005). Hedging the smirk, *Finance Research Letters* **2**(4): 195–200.

Bergman, Y. Z., Grundy, B. D. and Wiener, Z. (1996). General properties of option prices, *Journal of Finance* **51**: 1573–1610.

Bergomi, L. (2004). Smile dynamics, *RISK* **17**(9): 117–123.

Black, F. and Scholes, M. (1973). The pricing of options and corporate liabilities, *Journal of Political Economy* **81**: 637–654.

Bollen, N. and Whaley, R. E. (2004). Does net buying pressure affect the shape of the implied volatility functions?, *Journal of Finance* **59**(2): 711–753.

Bollerslev, T. and Todorov, V. (2011). Tails, fears, and risk premia, *Journal of Finance* **66**(6): 2165–2211.

Broadie, M., Chernov, M. and Johannes, M. (2007). Model specification and risk premia: Evidence from futures options, *Journal of Finance* **62**(3): 1453–1490.

Broadie, M., Chernov, M. and Johannes, M. (2009). Understanding index option returns, *Review of Financial Studies* **22**: 4493–4529.

Carr, P. and Madan, D. B. (1999). Option valuation using the fast Fourier transform, *Journal of Computational Finance* **2**(4): 61–73.

Carr, P. and Wu, L. (2007). Stochastic skew in currency options, *Journal of Financial Economics* **86**(1): 213–247.

Christoffersen, P., Feunou, B., Jacobs, K. and Meddahi, N. (2012). The economic value of realized volatility: Using high-frequency returns for option valuation, *Working paper*, Rotman School of Management, University of Toronto.

Christoffersen, P., Heston, S. and Jacobs, K. (2009). The shape and term structure of the index option smirk: Why multifactor stochastic volatility models work so well, *Management Science* **55**(12): 1914–1932.

Christoffersen, P. and Jacobs, K. (2004). Which GARCH model for option valuation?, *Management Science* **50**(9): 1204–1221.

Christoffersen, P., Jacobs, K. and Mimouni, K. (2010). Volatility dynamics for the S&P500: Evidence from realized volatility, daily returns and option prices, *Review of Financial Studies* **23**(8): 3141–3189.

Constantinides, G. M., Jackwerth, J. C. and Savov, A. (2011). The puzzle of index option returns, *Technical report*, Konstanz University.

Corsi, F., Fusari, N. and La Vecchia, D. (2013). Realizing smiles: Options pricing with realized volatility, *Journal of Financial Economics* **107**: 284–304.

Coval, J. D. and Shumway, T. (2001). Expected option returns, *Journal of Finance* **56**: 983–1009.

Cox, J. E. and Ross, S. A. (1976). The valuation of options for alternative stochastic processes, *Journal of Financial Economics* **76**: 145–166.

Dacorogna, M. M., Gençay, R., Müller, U., Olsen, R. B. and Pictet, O. V. (2001). *An Introduction to High-Frequency Finance*, Academic Press, London.

Dalang, R. C., Morton, A. and Willinger, W. (1990). Equivalent martingale measures and no-arbitrage in stochastic securities market models, *Stochastics* **29**: 185–201.

de Pooter, M., Martens, M. and van Dijk, D. (2008). Predicting the daily covariance matrix for S&P 100 stocks using intraday data – but which frequency to use?, *Econometric Reviews* **27**(1–3): 199–229.

Dumas, B., Fleming, J. and Whaley, R. E. (1998). Implied volatility functions: Empirical tests, *Journal of Finance* **53**(6): 2059–2106.

Dupire, B. (1994). Pricing with a smile, *RISK* **7**(1): 18–20.

Eraker, B. (2004). Do stock prices and volatility jump? reconciling evidence from spot and option prices, *Journal of Finance* **59**(3): 1367–1404.

Eurex Frankfurt AG (2009). Dow Jones EURO STOXX 50® INDEX Index Futures (FESX).
URL: *http://www.eurexchange.com/*

Ghysels, E., Harvey, A. and Renault, E. (1996). Stochastic volatility, *in* C. R. Rao and G. S. Maddala (eds), *Handbook of Statistics*, Vol. 14, North Holland, Amsterdam, chapter Statistical Methods in Finance, pp. 119–191.

Gouriéroux, C., Jasiak, J. and Sufana, R. (2009). The Wishart autoregressive processes of multivariate stochastic volatility, *Journal of Econometrics* **150**: 167–181.

Gruber, P., Tebaldi, C. and Trojani, F. (2010). Three make a dynamic smile – unspanned skewness and interacting volatility components in option valuation, *Technical report*, University of Lugano, Switzerland.

Han, B. (2008). Investor sentiment and option prices, *Review of Financial Studies* **21**: 387–414.

Hansen, P. R. and Lunde, A. (2006). Realised variance and market microstructure noise, *Journal of Business and Economic Statistics* **24**: 127–218.

Harvey, A., Ruiz, E. and Shephard, N. (1994). Multivariate stochastic variance models, *Review of Economic Studies* **61**: 247–264.

Heston, S. (1993). A closed-form solution for options with stochastic volatility with applications to bond and currency options, *Review of Financial Studies* **6**: 327–343.

Huang, J. Z. and Wu, L. (2004). Specification analysis of option pricing models based on time-changed Lévy processes, *Journal of Finance* **59**: 1405–1439.

Hull, J. and White, A. (1987). The pricing of options on assets with stochastic volatilities, *Journal of Finance* **42**: 281–300.

Jacod, J. and Shiryaev, A. (1987). *Limit Theorems for Stochastic Processes*, Springer-Verlag, Berlin.

Jiang, G. J. and Knight, J. L. (2002). Estimation of continuous-time processes via the empirical characteristic function, *Journal of Business and Economic Statistics* **20**(2): 198–212.

Jones, C. S. (2003). The dynamics of stochastic volatility: Evidence from underlying and options markets, *Journal of Econometrics* **116**: 181–224.

Jones, C. S. (2006). A nonlinear factor analysis of s&p 500 index option returns, *Journal of Finance* **61**: 2325–2363.

Karatzas, I. and Shreve, S. E. (1991). *Brownian Motion and Stochastic Calculus*, Springer-Verlag, Berlin, Heidelberg.

Kim, S., Shepard, N. and Chib, S. (1998). Stochastic volatility: Likelihood inference and comparison with ARCH models, *Review of Economic Studies* **65**: 361–393.

Pan, J. (2002). The jump-risk premia implicit in options: evidence from an integrated time-series study, *Journal of Financial Economics* **63**: 3–50.

Patton, A. (2011). Volatility forecast comparison using imperfect volatility proxies, *Journal of Econometrics* **160**(1): 246–256.

Poteshman, A. (2001). Underreaction, overreaction, and increasing misreaction to information in the option market, *Journal of Finance* **56**: 851–876.

Protter, P. E. (2005). *Stochastic Integration and Differential Equations*, 2nd edn, Springer-Verlag, Berlin, Heidelberg.

Renault, E. (1997). Econometric models of option pricing errors, *in* D. M. Kreps and K. F. Wallis (eds), *Advances in Economics and Econometrics, Seventh World Congress*, Econometric Society Monographs, Cambridge University Press, pp. 223–278.

Scott, L. (1987). Option pricing when the variance changes randomly: Theory, estimation, and an application, *Journal of Financial and Quantitative Analysis* **22**: 419–37.

Shepard, N. (1996). Statistical aspects of ARCH and stochastic volatility, *in* D. R. Cox, D. V. Hinkley and O. E. Barndorff-Nielsen (eds), *Time Series Models in Econometrics, Finance and Other Fields*, Chapman & Hall, London, pp. 1–67.

Stoxx Limited (2012). Factsheet: EURO STOXX 50® INDEX.
URL: *http://www.stoxx.com/indices/types/introduction.html*

Taylor, S. J. (1994). Modeling stochastic volatility: A review and comparative study, *Mathematical Finance* **4**: 183–204.

Todorov, V. and Tauchen, G. (2011). Volatility jumps, *Journal of Business and Economic Statistics* **29**(3): 356–371.

Todorov, V., Tauchen, G. and Grynkiv, I. (2011). Realized Laplace transforms for estimation of jump diffusive volatility models, *Technical report*, Duke University.

A Data filtering

Volkswagen squeeze out

We delete all trading days between October 27, 2008, and November 2, 2008, since during this time a squeeze out took place in Volkswagen AG, which is a major constituent of the EURO STOXX 50® . The squeeze-out was triggered after Porsche AG announced on October 26, 2008, that it increased its Volkswagen shares from 35% to 42.6% and that it possessed option rights to further increase its share to 74.1%. Since the Lower Saxony, a federal state of Germany, owns 20%, the free float of Volkswagen was only 6% of the total shares outstanding. However, at this time many market participants held speculative short positions on Volkswagen, which they were desperate to close.[23]

During the squeeze-out Volkswagen shares more than doubled and were traded in only low volumes. As a consequence, the no-arbitrage relationship between the index and the futures broke down. The situation continued for few days until index providers decided in an immediate action to reduce the fraction of Volkswagen for index calculation. This measure, which became effective on October 31, 2008, eased the situation. We decided to remove some additional days because it was only by 3 November that Volkswagen shares returned to levels they held prior to the squeeze.

Filtering RV data

For filtering RV data, we directly borrow from the established filtering steps used for stock price data as devised by Barndorff-Nielsen et al. (2009, Section 3) for TAQ data:

P1 Deletion of entries having a time stamp outside the time window the exchange is open. From July 1, 2003, to November 11, 2011, the EUREX trades OESX options from 09:00 to 17:30 CET. For FESX futures, there is also a pre-trading and a post-trading phase outside 09:00 to 17:30 CET, which by this choice is excluded from analysis.

P2 Deletion of zero prices. For EUREX data this applies when two market participants

[23] See `http://www.economist.com/node/12501847?story_id=12501847`.

trade with each other by mutually agreeing on a price, but without going through the order book. The trade is only routed via the EUREX trading system. This is done, for instance, in order to mitigate counterparty risk.[24] The price is not published and marked as zero in the record file, but the volume traded is known.

T2 Delete trades occurring in the post-trading period or within a trading halt.

T3 When multiple transactions have a common time stamp, use the median price.

T4/Q4 Delete entries for which the transaction price deviates by more than 10 mean absolute deviations from a running centered median computed from the 17 preceding and the 17 succeeding options (futures, index) observations, excluding the current one.[25]

Filtering calibration data

For calibration we apply the filtering rules P1, P2, and T2. Moreover we keep observations

1. within the implied volatility range of $[8\%; 80\%]$ (implied volatility filter);
2. within a (spot-)moneyness range of $[.99; 1.05]$ for calls and $[.95; 1.01]$ for puts (moneyness filter);
3. having at least five days, but less than 90 days to expiry (days to expiry filter).

These filters are standard in the literature working with daily option data to exclude observations that have unreasonably low and high implied volatility and that are thinly traded, see e.g. Bakshi et al. (2010). The time-to-maturity and strike filter is chosen to be very tight to avoid overstretching the ability of the Heston model to match the steep equity implied volatility smirk and the term structure of the implied volatility surface.

[24]When trades are routed via the EUREX trading system, counterparty risk remains with the exchange. EUREX hedges against this counterparty risk by asking for margin requirements in the form of selected collaterals, such as top-rated government bonds.

[25]For TAQ data, 25 is the original suggestion by Barndorff-Nielsen et al. (2009). We found that somewhat too large for options data.

Tables and Figures

Table 1: Simulation results for option realized variance

		BS model				Heston model							
						$I_1 + I_2 + 2I_3$				BS approximation			
		Put		Call		Put		Call		Put		Call	
Intra-day frq.	Quantile	β_0	β_1	β_0	β_1	β_0	β_1	β_0	β_1	β_0	β_1	β_0	β_1
	0.05	-0.0028	1.0044	-0.0029	1.0047	-0.0050	0.9955	-0.0059	0.8045	-0.0094	1.1207	-0.0053	0.3672
30 min.	0.50	-0.0014	1.0133	-0.0015	1.0131	-0.0014	1.0125	-0.0003	1.0050	0.0029	1.2547	0.0090	0.7140
	0.95	-0.0004	1.0244	-0.0004	1.0239	0.0010	1.0355	0.0321	1.0421	0.0097	1.4484	0.0813	0.9022
	0.05	-0.0015	1.0024	-0.0016	1.0024	-0.0028	0.9952	-0.0030	0.8413	-0.0068	1.1144	-0.0047	0.3722
15 min.	0.50	-0.0008	1.0069	-0.0008	1.0070	-0.0007	1.0060	0.0001	1.0001	0.0040	1.2394	0.0107	0.7148
	0.95	-0.0002	1.0126	-0.0002	1.0124	0.0009	1.0190	0.0256	1.0231	0.0103	1.4151	0.0805	0.8986
	0.05	-0.0005	1.0009	-0.0005	1.0009	-0.0014	0.9959	-0.0012	0.8270	-0.0062	1.1084	-0.0041	0.3785
5 min.	0.50	-0.0003	1.0024	-0.0003	1.0024	-0.0003	1.0020	0.0006	0.9957	0.0046	1.2347	0.0116	0.7046
	0.95	-0.0001	1.0042	-0.0001	1.0042	0.0007	1.0092	0.0288	1.0084	0.0104	1.4080	0.0784	0.8986

Option prices are simulated assuming the classic Black Scholes model (columns 3-6) and Heston model (columns 7-14) for the underlying price process. Observed (oRV) and model-based realized variances (RV) are computed using high-frequency returns at different frequencies: 30 minutes, 15 minutes, and 5 minutes. Results are reported by OLS regressions of oRV on a constant (β_0) and its underlying implied approximations (β_1) in terms of the 90% confidence intervals of the estimated coefficients that are obtained from 999 simulation runs. In the case of the Heston model, we report results assuming the correct Heston approximation (columns 7-10) and the wrong Black Scholes model (columns 11-14). All results are obtained by correctly adjusting time to expiry intra-day.

Table 2: Simulation results for option realized variance

		BS model				Heston model							
						$I_1 + I_2 + 2I_3$				BS approximation			
		Put		Call		Put		Call		Put		Call	
Intra-day frq.	Quantile	β_0	β_1	β_0	β_1	β_0	β_1	β_0	β_1	β_0	β_1	β_0	β_1
	0.05	-0.0010	0.9984	-0.0010	0.9987	-0.0026	0.9870	-0.0047	0.8160	-0.0063	1.1147	-0.0040	0.3716
30 min.	0.50	-0.0004	1.0031	-0.0004	1.0032	-0.0004	1.0027	0.0006	0.9949	0.0039	1.2413	0.0105	0.7015
	0.95	0.0001	1.0079	0.0001	1.0081	0.0019	1.0186	0.0275	1.0321	0.0104	1.4215	0.0751	0.8911
	0.05	-0.0005	0.9993	-0.0005	0.9993	-0.0017	0.9908	-0.0020	0.8558	-0.0051	1.1110	-0.0039	0.3790
15 min.	0.50	-0.0002	1.0017	-0.0002	1.0017	-0.0002	1.0011	0.0006	0.9950	0.0045	1.2340	0.0110	0.7082
	0.95	0.0000	1.0041	0.0001	1.0041	0.0013	1.0115	0.0222	1.0157	0.0106	1.4058	0.0726	0.8927
	0.0500	-0.0002	0.9998	-0.0002	0.9999	-0.0010	0.9944	-0.0008	0.8613	-0.0050	1.1079	-0.0037	0.3809
5 min.	0.5000	-0.0001	1.0006	-0.0001	1.0006	-0.0001	1.0003	0.0006	0.9946	0.0048	1.2339	0.0119	0.6993
	0.9500	0.0000	1.0014	0.0000	1.0014	0.0008	1.0068	0.0220	1.0067	0.0103	1.4054	0.0723	0.8951

Option prices are simulated assuming the classic Black Scholes model (columns 3-6) and Heston model (columns 7-14) for the underlying price process. Observed (oRV) and model-based realized variances (RV) are computed using high-frequency returns at different frequencies: 30 minutes, 15 minutes, and 5 minutes. Results are reported by OLS regressions of oRV on a constant (β_0) and its underlying implied approximations (β_1) in terms of the 90% confidence intervals of the estimated coefficients that are obtained from 999 simulation runs. In the case of the Heston model, we report results assuming the correct Heston approximation (columns 7-10) and the wrong Black Scholes model (columns 11-14). All results are obtained without adjusting time to expiry intra-day.

Summary statistics: RV data				
sample period	2003-2011		2003-2007	
	puts	calls	puts	calls
avg. # of options per day available for oRV	149	157	91	94
avg. # of options per day used for oRV	19	19	19	19
total # of oRV measures	1772	1836	933	983
avg. time to expiry (days)	16.5	16.5	16.5	16.5
avg. moneyness	0.971	1.025	0.981	1.015

Table 3: Summary statistics of observed realized variances (oRV) raw data after filtering. Statistics refer to most heavily traded calls and puts (fixed strike, fixed expiry date) from which daily oRV is computed. Two different time periods are considered: the whole sample (2003-2011) and the pre-financial crisis period only (2003-2007).

Summary statistics: calibration data				
sample period	2003-2011		2003-2007	
	A	B	A	B
total # of options	2.0×10^6	4.1×10^5	5.4×10^5	1.1×10^5
# of days in sample	2013	436	1044	213
avg. # of options per day	951	937	514	500
avg. time to expiry (days)	58	58	61	61
avg. moneyness	0.997	0.997	0.998	0.999

Table 4: Summary statistics of calibration data after filtering. Column B refers to the subsample used for estimating the structural parameters (only Wednesdays of original sample). Column A gives the statistics on the whole sample from which the Heston latent volatility series is calculated based on the structural parameter estimates. Two different time periods are considered: the whole sample (2003-2011) and the pre-financial crisis period only (2003-2007).

Heston calibration					
sample	κ^*	$\hat{\lambda}$	$\hat{\xi}$	$\hat{\rho}$	PE
2003-2011	2.0	0.0675	0.5197	-0.9012	8.31%
2003-2007	2.0	0.0532	0.4614	-0.8112	7.49%

Table 5: Calibrated parameters of the stochastic volatility Heston model: $dS(t)/S(t) = (r-d)dt + \sqrt{V(t)}dw_1(t),\ dV(t) = \kappa(\lambda - V(t))dt + \xi\sqrt{V(t)}dw_2(t),\ dw_1(t)dw_2(t) = \rho dt$. The starred parameter indicates that this parameter was held fixed during calibration. Column PE displays the average daily root mean squared relative pricing error computed at the strikes and time-to-maturities used for computing option realized variance. Two different time periods are considered: the whole sample (2003-2011) and the pre-financial crisis period only (2003-2007).

Puts									
	τ	3		5		8		10	
m		BS	Hes.	BS	Hes.	BS	Hes.	BS	Hes.
0.05	β_0	0.010	0.003	0.005	0.005	0.005	0.007	0.004	0.007
	SE	0.002	0.003	0.002	0.002	0.002	0.002	0.002	0.002
	β_1	1.078	0.980	1.138	0.902	1.134	0.865	1.157	0.845
	SE	0.023	0.028	0.025	0.028	0.031	0.031	0.036	0.036
	$\bar{R}^2$	0.901	0.768	0.903	0.803	0.892	0.784	0.885	0.778
	n	1471		1296		1210		1047	
0.10	β_0	0.012	0.010	0.009	0.010	0.008	0.012	0.007	0.011
	SE	0.002	0.003	0.002	0.002	0.002	0.002	0.002	0.002
	β_1	1.068	0.968	1.098	0.894	1.106	0.864	1.123	0.848
	SE	0.022	0.027	0.029	0.026	0.027	0.029	0.031	0.034
	$\bar{R}^2$	0.893	0.724	0.885	0.770	0.880	0.754	0.875	0.751
	n	1707		1522		1431		1249	
0.15	β_0	0.012	0.014	0.009	0.015	0.009	0.016	0.007	0.015
	SE	0.002	0.003	0.002	0.003	0.002	0.003	0.002	0.003
	β_1	1.070	0.955	1.103	0.879	1.107	0.847	1.125	0.829
	SE	0.022	0.026	0.029	0.026	0.027	0.029	0.030	0.034
	$\bar{R}^2$	0.892	0.702	0.884	0.729	0.878	0.718	0.872	0.700
	n	1772		1587		1493		1310	

Table 6: Put options regression results: We consider regressing $\text{oRV} = \beta_0 + \beta_1 \text{dRV}$, where dRV are based on the Black-Scholes (BS) and the Heston (H) model for various moneyness (m) and time-to-maturity filters (τ). SE denotes Newey-West standard errors and n the sample size. For example, panel $\tau = 5, m = 0.1$ refers to a regression executed on data *including* all options with $m \leq 0.1$ and $5 < \tau \leq 35$ days. The data spans the time period from 2003 to 2011.

		Calls							
	τ	3		5		8		10	
m		BS	Hes.	BS	Hes.	BS	Hes.	BS	Hes.
	β_0	0.020	0.034	0.019	0.031	0.018	0.029	0.022	0.029
	SE	0.003	0.003	0.003	0.003	0.004	0.004	0.004	0.005
0.05	β_1	0.685	0.809	0.672	0.774	0.668	0.785	0.619	0.754
	SE	0.020	0.032	0.028	0.036	0.033	0.043	0.044	0.068
	$\bar{R}^2$	0.843	0.733	0.820	0.743	0.812	0.736	0.761	0.663
	n	1606		1423		1332		1143	
	β_0	0.023	0.041	0.023	0.039	0.022	0.037	0.025	0.038
	SE	0.003	0.004	0.003	0.004	0.003	0.004	0.003	0.004
0.10	β_1	0.647	0.717	0.626	0.670	0.626	0.673	0.582	0.623
	SE	0.022	0.035	0.026	0.037	0.027	0.040	0.030	0.043
	$\bar{R}^2$	0.820	0.684	0.797	0.699	0.800	0.703	0.768	0.655
	n	1804		1618		1522		1327	
	β_0	0.024	0.042	0.024	0.040	0.022	0.038	0.025	0.039
	SE	0.003	0.004	0.003	0.004	0.003	0.004	0.003	0.004
0.15	β_1	0.641	0.703	0.622	0.657	0.621	0.656	0.582	0.610
	SE	0.022	0.036	0.026	0.037	0.026	0.041	0.029	0.044
	$\bar{R}^2$	0.82	0.682	0.8	0.701	0.805	0.706	0.775	0.663
	n	1836		1649		1553		1356	

Table 7: Call options regression results: We consider regressing oRV $= \beta_0 + \beta_1$dRV, where dRV are based on the Black-Scholes (BS) and the Heston (H) model for various moneyness (m) and time-to-maturity filters (τ). SE denotes Newey-West standard errors and n the sample size. For example, panel $\tau = 5, m = 0.1$ refers to a regression executed on data *including* all options with $m \leq 0.1$ and $5 < \tau \leq 35$ days. The data spans the time period from 2003 to 2011.

Additional regressors: Puts

	all data						low vol.		high vol.		low vol.		high vol.	
	BS	Hes.	BS	Hes.	BS	Hes.	BS	Hes.	BS	Hes.	BS	Hes.	BS	Hes.
β_0	0.009	0.010					0.009	0.012	0.020	0.024				
SE	0.002	0.002					0.001	0.002	0.005	0.004				
β_1	1.098	0.894	1.093	0.850	1.046	0.792	1.035	0.758	1.101	0.988	0.998	0.673	1.038	0.876
SE	0.029	0.026	0.033	0.029	0.033	0.028	0.021	0.023	0.049	0.034	0.025	0.023	0.056	0.038
τ			-0.053	-0.509	-0.153	-0.640					-0.130	-0.584	-0.439	-1.137
SE			0.060	0.082	0.067	0.082					0.051	0.060	0.172	0.212
m			0.013	0.041	0.016	0.042					0.011	0.028	0.042	0.082
SE			0.005	0.006	0.006	0.006					0.004	0.005	0.014	0.015
RV					52.722	113.479					173.385	504.349	36.567	63.508
SE					14.601	22.419					33.481	41.990	16.147	19.886
$\bar{R}^2$	0.885	0.770	0.885	0.778	0.893	0.818	0.899	0.807	0.859	0.776	0.901	0.850	0.866	0.813
n	1522		1522		1522		1054		468		1054		468	

Table 8: Put options regression results: We consider regressing oRV = $\beta_0 + \beta_1$dRV + add. reg., where dRV are based on the Black-Scholes (BS) and the Heston (H) model, and add. reg. denotes the additional regressors: moneyness m, time to maturity τ, and underlying's RV computed using 5 minute returns. SE denotes Newey-West standard errors and n the sample size. Low (high) volatility regime refers to days where the RV of the underlying index is smaller (larger) than 0.01, see Figure 2. The data spans the time period between 2003 and 2011.

Additional regressors: Calls

	all data						low vol.		high vol.		low vol.		high vol.	
	BS	Hes.	BS	Hes.	BS	Hes.	BS	Hes.	BS	Hes.	BS	Hes.	BS	Hes.
β_0	0.023	0.039					0.012	0.022	0.034	0.048				
SE	0.003	0.004					0.003	0.003	0.006	0.007				
β_1	0.626	0.670	0.592	0.618	0.600	0.654	0.738	0.915	0.562	0.583	0.714	0.931	0.528	0.548
SE	0.026	0.037	0.028	0.039	0.030	0.044	0.028	0.039	0.034	0.046	0.033	0.050	0.037	0.052
τ			-0.545	-0.707	-0.524	-0.632					-0.323	-0.226	-0.650	-0.721
SE			0.075	0.097	0.074	0.101					0.058	0.084	0.175	0.203
m			0.054	0.078	0.053	0.075					0.035	0.048	0.070	0.090
SE			0.007	0.008	0.006	0.008					0.005	0.007	0.014	0.016
RV					-16.015	-46.997					-98.370	-362.687	3.122	-12.911
SE					21.310	29.813					52.521	72.369	26.809	34.356
$\bar{R}^2$	0.797	0.699	0.806	0.715	0.806	0.718	0.801	0.718	0.774	0.684	0.806	0.730	0.781	0.693
n	1618		1618		1618		1121		497		1121		497	

Table 9: Call options regression results: We consider regressing oRV $= \beta_0 + \beta_1$dRV + add. reg., where dRV are based on the Black-Scholes (BS) and the Heston (H) model, and add. reg. denotes the additional regressors: moneyness m, time to maturity τ, and underlying's RV computed using 5 minute returns. SE denotes Newey-West standard errors and n the sample size. Low (high) volatility regime refers to days where the RV of the underlying index is smaller (larger) than 0.01, see Figure 2. The data spans the time period between 2003 and 2011.

Non-crisis period: Puts									
	τ	3		5		8		10	
m		BS	Hes.	BS	Hes.	BS	Hes.	BS	Hes.
0.05	β_0	0.009	0.003	0.006	0.005	0.007	0.008	0.007	0.008
	SE	0.002	0.003	0.002	0.002	0.002	0.002	0.002	0.002
	β_1	1.050	0.938	1.083	0.865	1.062	0.820	1.061	0.793
	SE	0.032	0.033	0.029	0.028	0.034	0.028	0.040	0.033
	$\bar{R}^2$	0.896	0.815	0.900	0.840	0.890	0.833	0.877	0.821
	n	884		785		737		643	
0.10	β_0	0.011	0.006	0.010	0.008	0.008	0.010	0.008	0.009
	SE	0.003	0.003	0.003	0.002	0.002	0.002	0.002	0.002
	β_1	1.028	0.925	1.035	0.852	1.050	0.810	1.041	0.792
	SE	0.035	0.033	0.044	0.029	0.033	0.029	0.038	0.033
	$\bar{R}^2$	0.887	0.789	0.880	0.800	0.883	0.805	0.875	0.803
	n	927		827		777		681	
0.15	β_0	0.011	0.008	0.010	0.010	0.008	0.012	0.008	0.011
	SE	0.003	0.004	0.003	0.003	0.002	0.003	0.002	0.002
	β_1	1.029	0.918	1.038	0.842	1.054	0.801	1.047	0.779
	SE	0.034	0.034	0.042	0.029	0.033	0.029	0.038	0.035
	$\bar{R}^2$	0.887	0.774	0.881	0.774	0.885	0.770	0.877	0.750
	n	933		833		782		686	

Table 10: Put options regression results: We consider regressing oRV $= \beta_0 + \beta_1$dRV, where dRV are based on the Black-Scholes (BS) and the Heston (H) model for various moneyness (m) and time-to-maturity filters (τ). SE denotes Newey-West standard errors and n the sample size. For example, panel $\tau = 5, m = 0.1$ refers to a regression executed on data *including* all options with $m \leq 0.1$ and $5 < \tau \leq 35$ days. The data spans the time period from 2003 to 2007.

Non-crisis period: Calls									
	τ	3		5		8		10	
m		BS	Hes.	BS	Hes.	BS	Hes.	BS	Hes.
0.05	β_0	0.015	0.023	0.016	0.024	0.016	0.024	0.016	0.022
	SE	0.002	0.004	0.003	0.003	0.002	0.003	0.003	0.003
	β_1	0.756	0.909	0.732	0.840	0.718	0.823	0.712	0.847
	SE	0.022	0.042	0.031	0.045	0.026	0.040	0.029	0.044
	$\bar{R}^2$	0.844	0.750	0.807	0.750	0.802	0.740	0.748	0.684
	n	957		854		803		697	
0.10	β_0	0.016	0.025	0.017	0.026	0.016	0.025	0.015	0.024
	SE	0.003	0.004	0.003	0.003	0.002	0.003	0.003	0.003
	β_1	0.747	0.883	0.721	0.815	0.720	0.806	0.717	0.815
	SE	0.023	0.043	0.030	0.046	0.024	0.043	0.028	0.041
	$\bar{R}^2$	0.837	0.743	0.799	0.744	0.805	0.743	0.759	0.694
	n	983		880		828		722	
0.15	β_0	0.016	0.025	0.017	0.026	0.016	0.025	0.015	0.024
	SE	0.003	0.004	0.003	0.003	0.002	0.003	0.003	0.003
	β_1	0.747	0.883	0.721	0.815	0.720	0.806	0.717	0.815
	SE	0.023	0.043	0.030	0.046	0.024	0.043	0.028	0.041
	$\bar{R}^2$	0.837	0.743	0.799	0.744	0.805	0.743	0.759	0.694
	n	983		880		828		722	

Table 11: Call options regression results: We consider regressing oRV $= \beta_0 + \beta_1$dRV, where dRV are based on the Black-Scholes (BS) and the Heston (H) model for various moneyness (m) and time-to-maturity filters (τ). SE denotes Newey-West standard errors and n the sample size. For example, panel $\tau = 5, m = 0.1$ refers to a regression executed on data *including* all options with $m \leq 0.1$ and $5 < \tau \leq 35$ days. The data spans the time period from 2003 to 2007.

Type II violations: Puts									
	τ	3		5		8		10	
m		BS	Hes.	BS	Hes.	BS	Hes.	BS	Hes.
0.05	β_0	0.012	0.002	0.005	0.003	0.004	0.004	0.002	0.004
	SE	0.003	0.004	0.002	0.002	0.003	0.003	0.002	0.004
	β_1	1.096	1.052	1.172	0.987	1.184	0.963	1.223	0.948
	SE	0.029	0.032	0.029	0.03	0.038	0.04	0.041	0.052
	$\bar{R}^2$	0.897	0.774	0.901	0.818	0.887	0.783	0.885	0.786
	n	949		818		759		639	
0.10	β_0	0.012	0.008	0.007	0.007	0.007	0.008	0.005	0.007
	SE	0.002	0.004	0.002	0.002	0.002	0.003	0.003	0.003
	β_1	1.103	1.04	1.157	0.98	1.162	0.962	1.191	0.95
	SE	0.026	0.03	0.027	0.027	0.034	0.034	0.037	0.041
	$\bar{R}^2$	0.896	0.742	0.897	0.806	0.886	0.772	0.888	0.785
	n	1077		941		881		752	
0.15	β_0	0.012	0.01	0.007	0.009	0.007	0.01	0.005	0.009
	SE	0.002	0.004	0.002	0.002	0.002	0.003	0.003	0.003
	β_1	1.107	1.036	1.165	0.976	1.166	0.956	1.198	0.945
	SE	0.026	0.03	0.029	0.027	0.034	0.034	0.037	0.041
	$\bar{R}^2$	0.896	0.727	0.898	0.774	0.884	0.757	0.886	0.761
	n	1103		967		906		777	

Table 12: Put options regression results: We consider regressing oRV $= \beta_0 + \beta_1$dRV, where dRV are based on the Black-Scholes (BS) and the Heston (H) model for various moneyness (m) and time-to-maturity filters (τ). SE denotes Newey-West standard errors and n the sample size. For example, panel $\tau = 5, m = 0.1$ refers to a regression executed on data *including* all options with $m \leq 0.1$ and $5 < \tau \leq 35$ days. We exclude days with more than one violation of type II (that is underlying index changing while simultaneously the put price remains unchanged) according to the definition introduced in Bakshi et al. (2000a). The data spans the time period from 2003 to 2011.

Type II violations: Calls									
	τ	3		5		8		10	
m		BS	Hes.	BS	Hes.	BS	Hes.	BS	Hes.
0.05	β_0	0.019	0.026	0.018	0.026	0.019	0.026	0.022	0.026
	SE	0.004	0.004	0.005	0.005	0.006	0.006	0.007	0.008
	β_1	0.698	0.851	0.687	0.795	0.664	0.781	0.62	0.758
	SE	0.027	0.039	0.039	0.047	0.044	0.056	0.062	0.094
	$\bar{R}^2$	0.869	0.784	0.848	0.796	0.848	0.795	0.808	0.733
	n	1023		894		829		694	
0.10	β_0	0.021	0.033	0.02	0.033	0.021	0.033	0.024	0.035
	SE	0.004	0.004	0.004	0.004	0.005	0.004	0.005	0.004
	β_1	0.669	0.772	0.656	0.712	0.636	0.69	0.596	0.64
	SE	0.025	0.034	0.033	0.036	0.035	0.037	0.041	0.042
	$\bar{R}^2$	0.855	0.744	0.838	0.764	0.842	0.766	0.821	0.73
	n	1137		1006		938		800	
0.15	β_0	0.022	0.034	0.021	0.033	0.022	0.034	0.024	0.035
	SE	0.004	0.004	0.004	0.004	0.004	0.004	0.005	0.004
	β_1	0.664	0.761	0.65	0.703	0.631	0.682	0.596	0.64
	SE	0.025	0.034	0.032	0.034	0.034	0.035	0.039	0.04
	$\bar{R}^2$	0.855	0.745	0.84	0.769	0.845	0.773	0.826	0.741
	n	1153		1022		954		814	

Table 13: Call options regression results: We consider regressing oRV $= \beta_0 + \beta_1$dRV, where dRV are based on the Black-Scholes (BS) and the Heston (H) model for various moneyness (m) and time-to-maturity filters (τ). SE denotes Newey-West standard errors and n the sample size. For example, panel $\tau = 5, m = 0.1$ refers to a regression executed on data *including* all options with $m \leq 0.1$ and $5 < \tau \leq 35$ days. We exclude days with more than one violation of type II (that is underlying index changing while simultaneously the call price remains unchanged) according to the definition introduced in Bakshi et al. (2000a). The data spans the time period from 2003 to 2011.

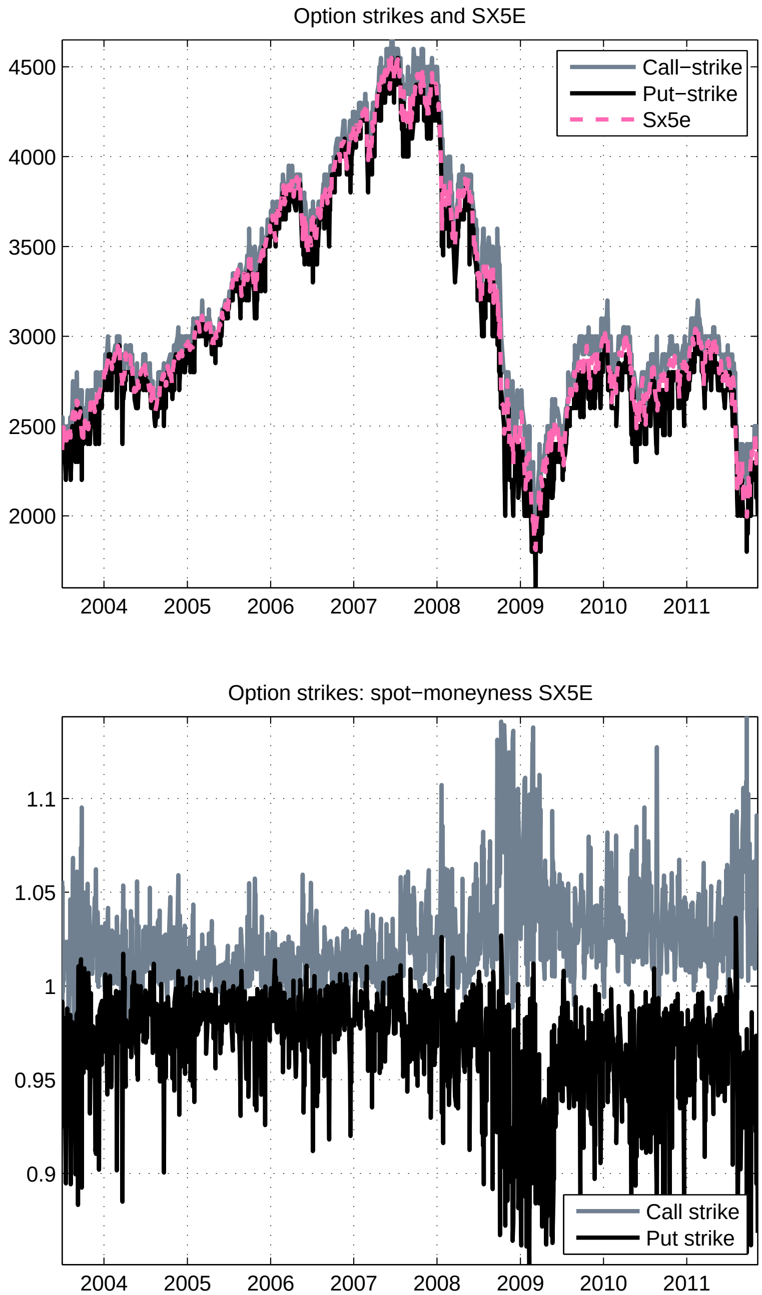

Figure 1: Characteristics of the considered options. Top panel: the EURO STOXX 50® is shown along with selected strikes. Bottom panel: the moneyness series of the selected options is plotted.

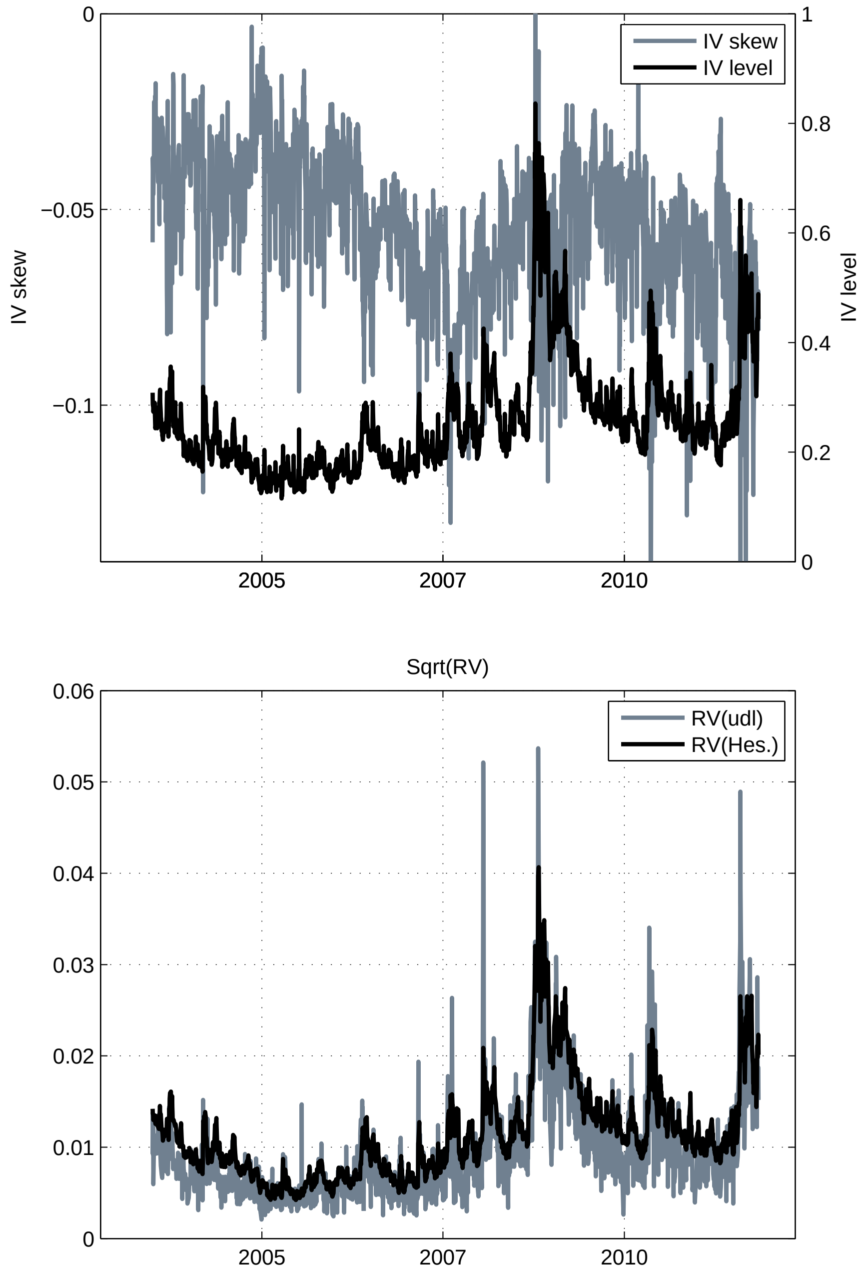

Figure 2: Top panel: Daily at-the-money BS implied volatility (IV) level (right axis) and daily implied volatility (IV) skew (left axis) time series. IV skew is defined as $\hat{\sigma}_{1.05} - \hat{\sigma}_{0.95}$ at 15 days to expiry. Bottom panel: Option-implied underlying (daily) RV obtained from the calibration of the Heston model superimposed on the RV computed using 5 minutes returns of the underlying EURO STOXX 50® index. The sample spans the time period from 2003 to 2011.

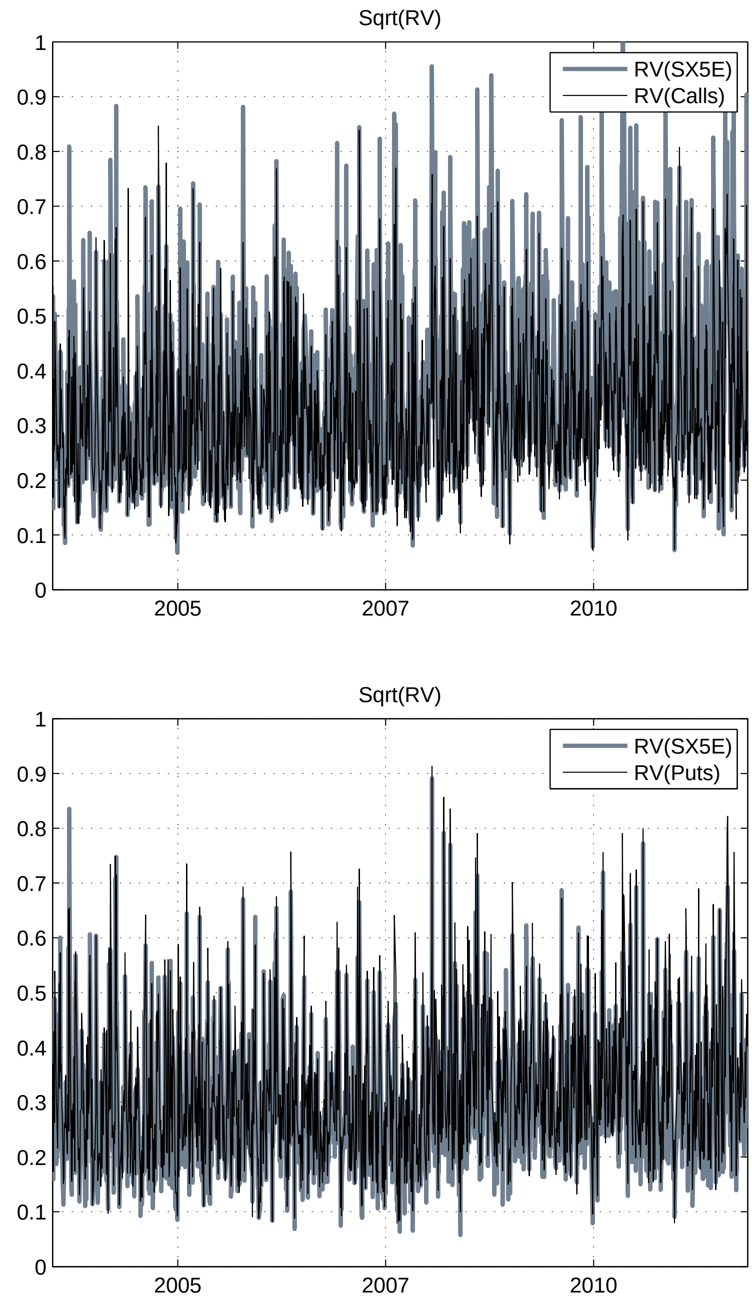

Figure 3: Daily time series of observed option realized volatilities (oRV) superimposed on realized volatilities computed assuming the classic one-factor Black and Scholes (BS) model for the underlying index.

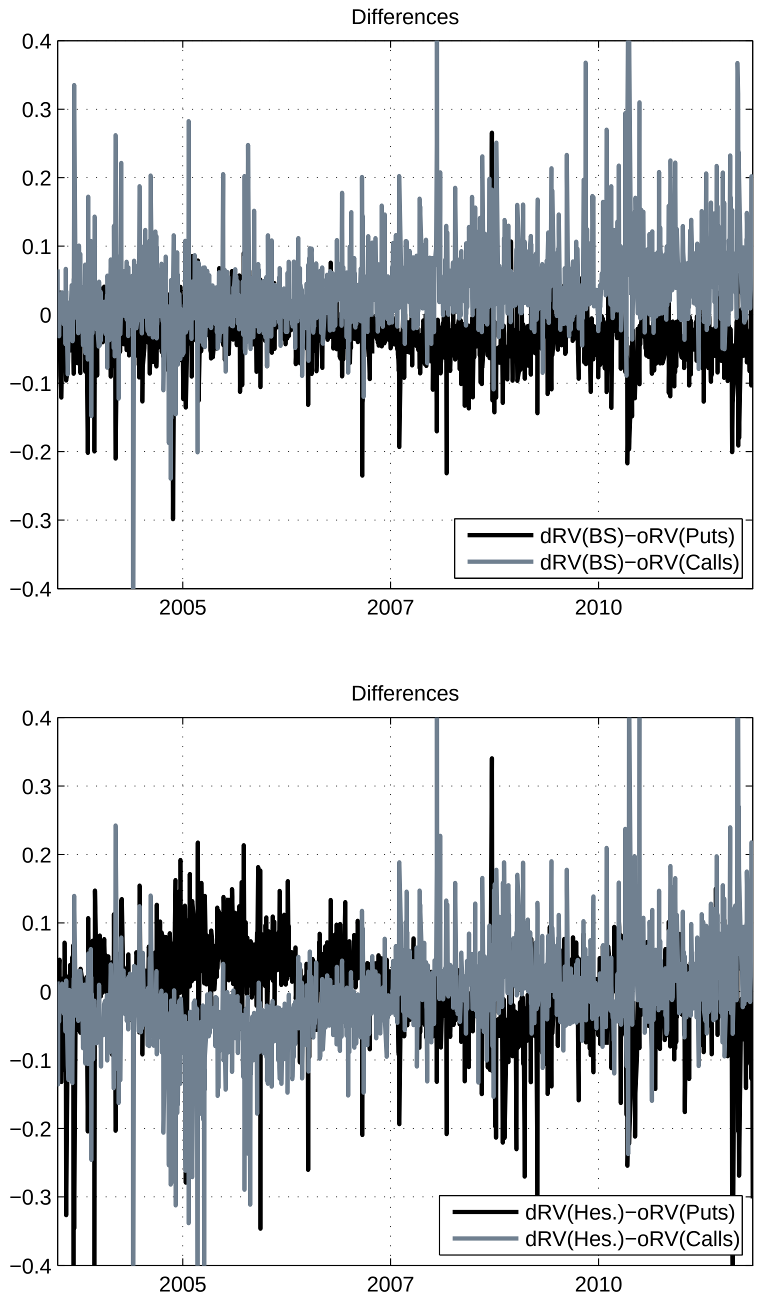

Figure 4: Time series of the differences between underlying-implied option realized volatility and observed option realized volatility (oRV). The data spans the time period from 2003 to 2011. Top panel: underlying-implied option realized volatility based on the BS model (dRV(BS)). Bottom panel: underlying-implied option realized volatility based on the Heston model (dRV(Heston)).

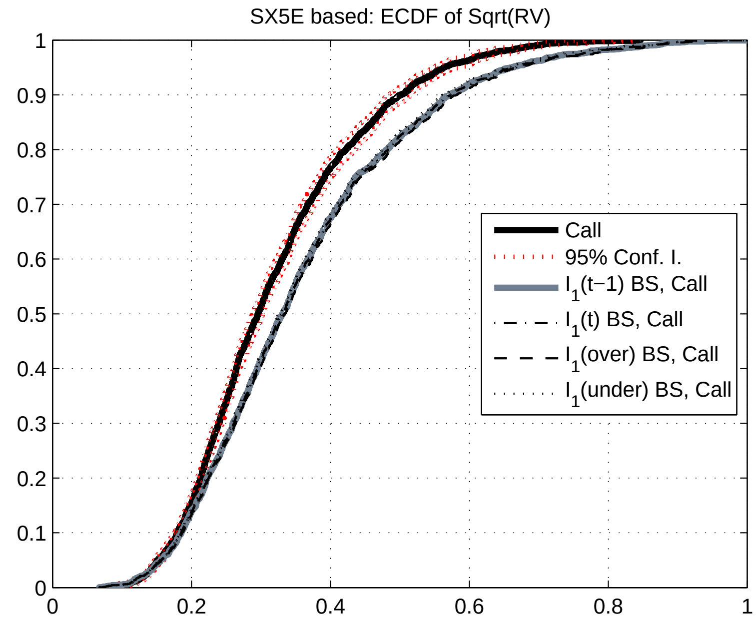

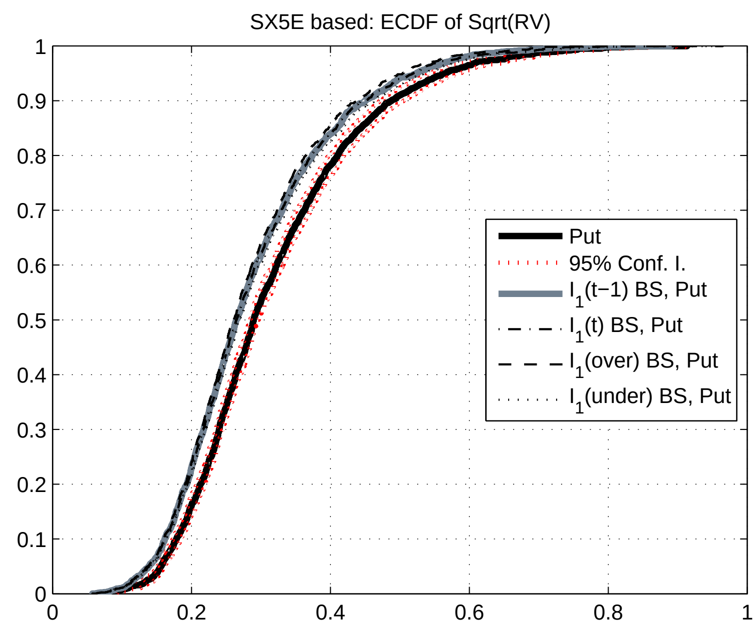

Figure 5: Empirical cumulative distribution function (CDF) of option RV obtained from high-frequency data (black, solid) and BS-based approximations. Shown are four approximations: the estimator based on the Itô discretization at the beginning of the period (at $t-1$, grey, solid); an estimate evaluated at the end of the period (at t, black, dashed-dotted); two estimates with evaluation times conditionally on the sign of the return leading to an over/under-estimate (black, dashed / black, dotted). Red dotted lines indicate the 95% confidence interval for the CDF. The data spans the time period from 2003 to 2011.

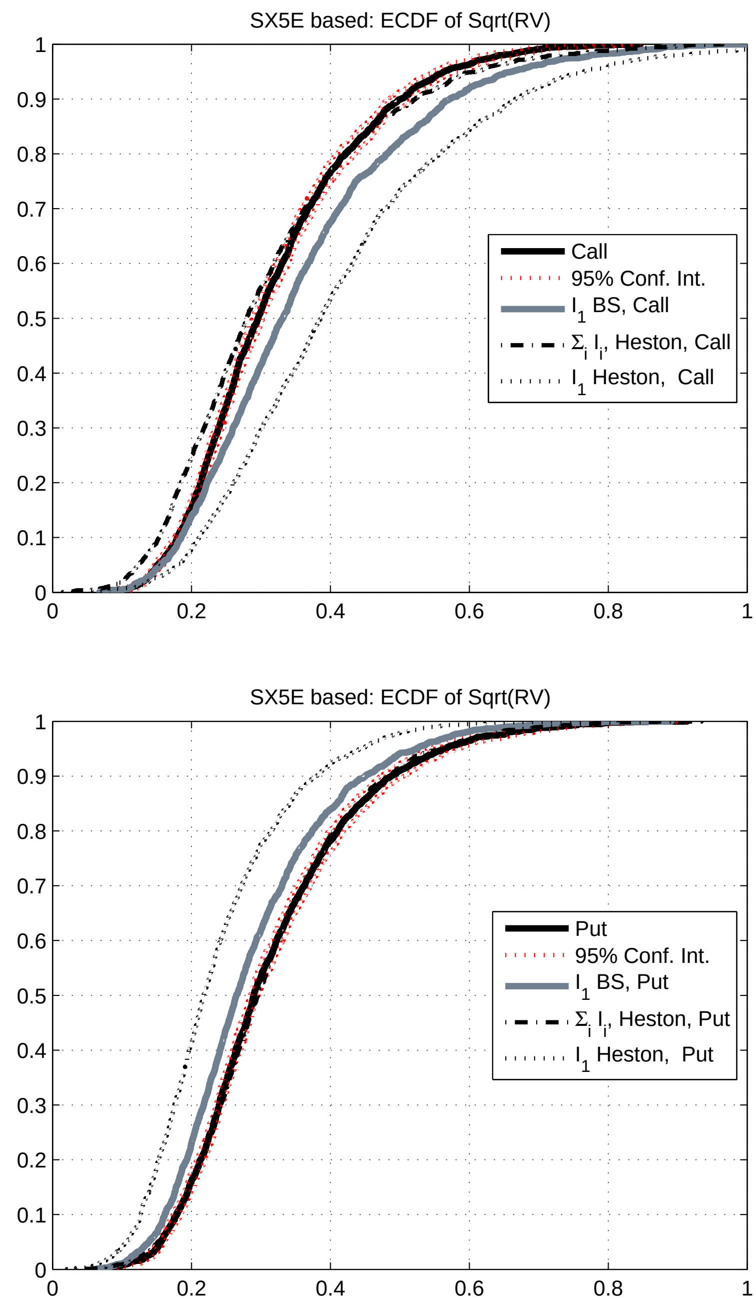

Figure 6: Empirical cumulative distribution function (CDF) of option RV obtained from high-frequency data (black, solid), together with dotted lines for the 95% confidence bounds, superimposed on: (i) the full Heston-based RV including all three integral terms (dotted-dashed lines); (ii) the Heston-based RV using solely the first term, similarly to the BS case (dotted lines); and (iii) the BS-based RV CDFs (solid, grey lines). The data spans the time period from 2003 to 2011.

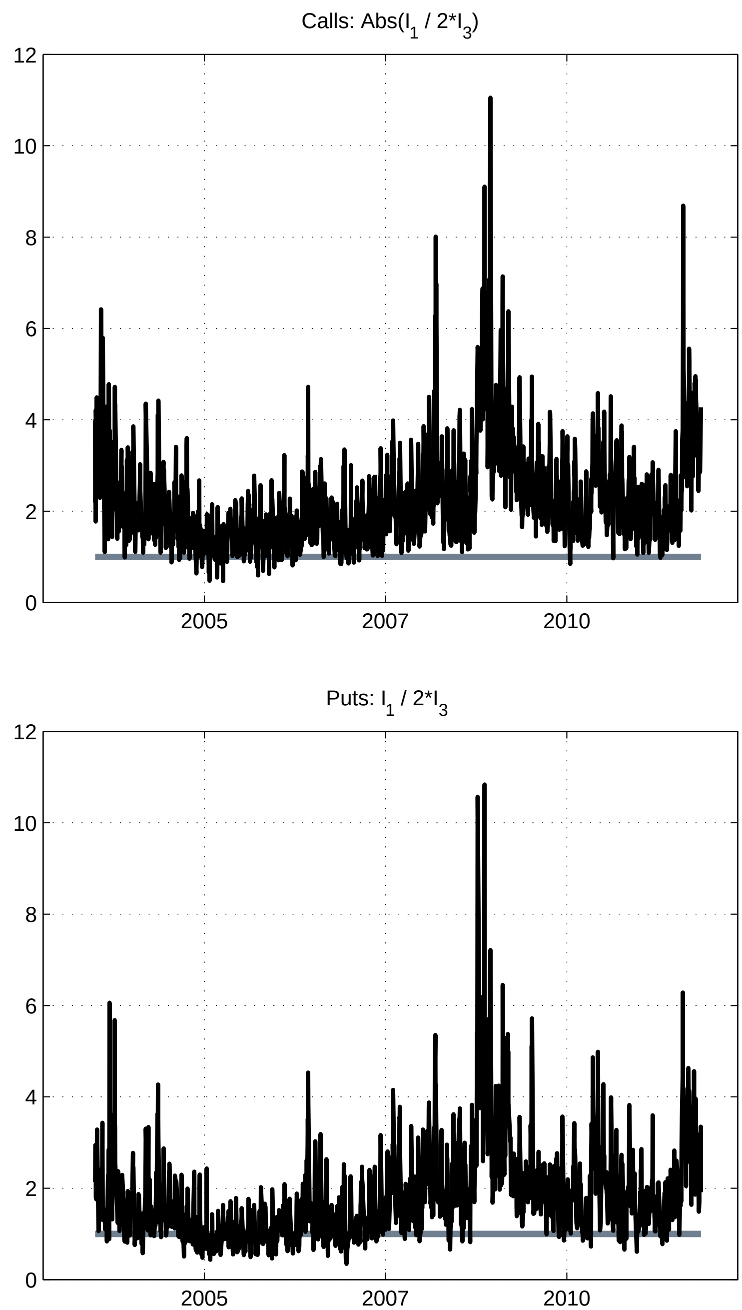

Figure 7: Relative importance of I_3 in comparison to I_1 for the computation of Heston-based RV. The grey solid line indicates one, i.e., when both terms are of equal size. The data spans the time period from 2003 to 2011.

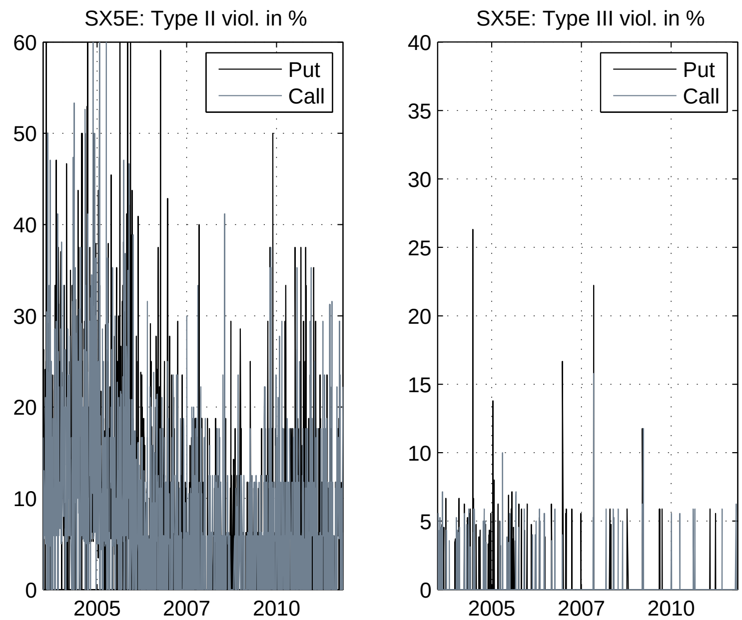

Figure 8: Time series of the frequencies of daily observed violations of the properties shared by one-dimensional diffusion models according to the definition given in Bakshi et al. (2000a): Type II violations are defined as changes in the underlying index EURO STOXX 50® (SX5E) with simultaneous prices of options remaining unchanged. Type III violations are changes in the option prices when the underlying index remains unchanged. The data spans the time period from 2003 to 2011.